Klimaänderung I
1. Rahmen, Kontext, Methoden

Robert Sausen

Institut für Physik der Atmosphäre
Deutsches Zentrum für Luft- und Raumfahrt
Oberpfaffenhofen

Vorlesung WS 2021/22

LMU München

DLR

Technical information

- http://www.pa.op.dlr.de/~RobertSausen/vorlesung/index.html
  - Most recent update on the lecture
  - Slides of the lecture (with some delay)

  - See also LSF https://lsf.verwaltung.uni-muenchen.de/

- Contact: robert.sausen@dlr.de

- Further information:
  - www.ipcc.ch
  - www.de-ipcc.de

Contents of IPCC AR 6 2021
Working Group I: the Physical Science Basis

Chapters

Chapter 1: Framing, context, methods	DOWNLOAD
Chapter 2: Changing state of the climate system	DOWNLOAD
Chapter 3: Human influence on the climate system	DOWNLOAD
Chapter 4: Future global climate: scenario-based projections and near-term information	DOWNLOAD
Chapter 5: Global carbon and other biogeochemical cycles and feedbacks	DOWNLOAD
Chapter 6: Short-lived climate forcers	DOWNLOAD
Chapter 7: The Earth's energy budget, climate feedbacks, and climate sensitivity	DOWNLOAD
Chapter 8: Water cycle changes	DOWNLOAD
Chapter 9: Ocean, cryosphere, and sea level change	DOWNLOAD
Chapter 10: Linking global to regional climate change	DOWNLOAD
Chapter 11: Weather and climate extreme events in a changing climate	DOWNLOAD
Chapter 12: Climate change information for regional impact and for risk assessment	DOWNLOAD
Atlas	DOWNLOAD

Supplementary Material

Annexes

https://www.ipcc.ch/report/ar6/wg1/#FullReport

Chapter 1: Framing, context, and methods

Coordinating Lead Authors:

Deliang Chen (Sweden), Maisa Rojas (Chile), Bjørn H. Samset (Norway)

Lead Authors:

Kim Cobb (United States of America), Aida Diongue-Niang (Senegal), Paul Edwards (United States of America), Seita Emori (Japan), Sergio Henrique Faria (Spain/Brazil), Ed Hawkins (United Kingdom), Pandora Hope (Australia), Philippe Huybrechts (Belgium), Malte Meinshausen (Australia/Germany), Sawsan Khair Elsied Abdel Rahim Mustafa (Sudan), Gian-Kasper Plattner (Switzerland), Anne Marie Treguier (France)

IPCC AR6 WG I, 2021, Chapter 1

Chapter 1: Framing, context, and methods

Contributing Authors:

Hui-Wen Lai (Sweden), Tania Villaseñor (Chile), Rondrotiana Barimalala (South Africa/Madagascar), Rosario Carmona (Chile), Peter M. Cox (United KingdomK), Wolfgang Cramer (France/Germany), Francisco J. Doblas-Reyes (Spain), Hans Dolman (The Netherlands), Alessandro Dosio (Italy), Veronika Eyring (Germany), Gregory M. Flato (Canada), Piers Forster (United Kingdom), David Frame (New Zealand), Katja Frieler (Germany), Jan S. Fuglestvedt (Norway), John C. Fyfe (Canada), Mathias Garschagen (Germany), Joelle Gergis (Australia), Nathan P. Gillett (Canada), Michael Grose (Australia), Eric Guilyardi (France), Celine Guivarch (France), Susan Hassol (United States of America), Zeke Hausfather (United States of America), Hans Hersbach (United Kingdom/The Netherlands), Helene T. Hewitt (United Kingdom), Mark Howden (Australia), Christian Huggel (Switzerland), Margot Hurlbert (Canada), Christopher Jones (United Kingdom), Richard G. Jones (United Kingdom), Darrell S. Kaufman (United States of America), Robert E. Kopp (United States of America), Anthony Leiserowitz (United States of America), Robert J. Lempert (United States of America), Jared Lewis (Australia/New Zealand), Hong Liao (China), Nikki Lovenduski (United States of America), Marianne T. Lund (Norway), Katharine Mach (United States of America), Douglas Maraun (Austria/Germany), Jochem Marotzke (Germany), Jan Minx (Germany), Zebedee R.J. Nicholls (Australia), Brian C. O'Neill (United States of America), M. Giselle Ogaz (Chile), Friederike Otto (United Kingdom /Germany), Wendy Parker (United Kingdom), Camille Parmesan (France, United Kingdom/United States of America), Warren Pearce (United Kingdom), Roque Pedace (Argentina), Andy Reisinger (New Zealand), James Renwick (New Zealand), Keywan Riahi (Austria), Paul Ritchie (United Kingdom), Joeri Rogelj (United Kingdom/Belgium), Rodolfo Sapiains (Chile), Yusuke Satoh (Japan), Sonia I. Seneviratne (Switzerland), Theodore G. Shepherd (United Kingdom/Canada), Jana Sillmann (Norway/Germany), Lucas Silva (Portugal/Switzerland), Aimée B.A. Slangen (The Netherlands), Anna A. Sörensson (Argentina), Peter Steinle (Australia), Thomas F. Stocker (Switzerland), Martina Stockhause (Germany), Daithi Stone (New Zealand), Abigail Swann (United States of America), Sophie Szopa (France), Izuru Takayabu (Japan), Claudia Tebaldi (United States of America), Laurent Terray (France), Peter W. Thorne (Ireland/ United Kingdom), Blair Trewin (Australia), Isabel Trigo Portugal), Maarten K. van Aalst (The Netherlands), Bart van den Hurk (The Netherlands), Detlef van Vuuren (The Netherlands), Robert Vautard (France), Carolina Vera (Argentina), David Viner (United Kingdom), Axel von Engeln (Germany), Karina von Schuckmann (France/Germany), Xuebin Zhang (Canada)

IPCC AR6 WG I, 2021, Chapter 1

Chapter 1: Framing, context, and methods

Review Editors:

Nares Chuersuwan (Thailand), Gabriele Hegerl (United Kingdom/Germany), Tetsuzo Yasunari (Japan)

IPCC AR6 WG I, 2021, Chapter 1

Statements in the Executive Summary

Working Group I (WGI) of the Intergovernmental Panel on Climate Change (IPCC) assesses the current evidence on the physical science of climate change, evaluating knowledge gained from observations, reanalyses, paleoclimate archives and climate model simulations, as well as physical, chemical and biological climate processes. This chapter sets the scene for the WGI assessment, placing it in the context of ongoing global and regional changes, international policy responses, the history of climate science and the evolution from previous IPCC assessments, including the Special Reports prepared as part of this Assessment Cycle. Key concepts and methods, relevant recent developments, and the modelling and scenario framework used in this assessment are presented.

IPCC 2021, Chap. 1

Statements in the Executive Summary

Framing and Context of the WGI Report (1)

The WGI contribution to the IPCC Sixth Assessment Report (AR6) assesses new scientific evidence relevant for a world whose climate system is rapidly changing, overwhelmingly due to human influence. The five IPCC assessment cycles since 1990 have comprehensively and consistently laid out the rapidly accumulating evidence of a changing climate system, with the Fourth Assessment Report (AR4, 2007) being the first to conclude that warming of the climate system is unequivocal. Sustained changes have been documented in all major elements of the climate system, including the atmosphere, land, cryosphere, biosphere and ocean. Multiple lines of evidence indicate the unprecedented nature of recent large-scale climatic changes in context of all human history, and that they represent a millennial-scale commitment for the slow-responding elements of the climate system, resulting in continued worldwide loss of ice, increase in ocean heat content, sea level rise and deep ocean acidification. {1.2.1, 1.3, Box 1.2, Appendix 1.A}

IPCC 2021, Chap. 1

The structure of the AR6 WGI Report

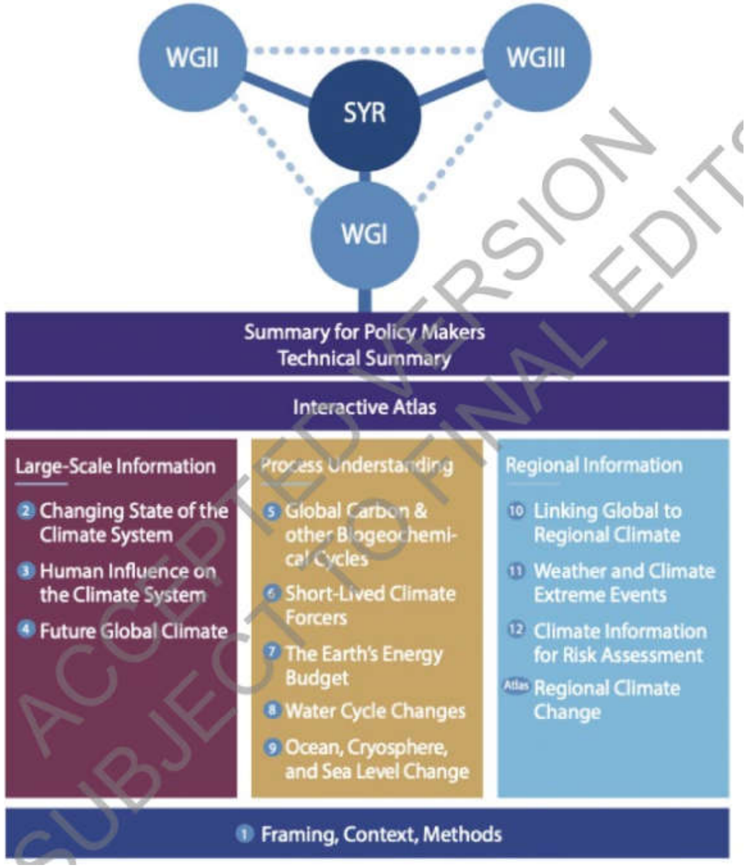

Figure 1.1: The structure of the AR6 WGI Report. Shown are the three pillars of AR6 WGI, its relation to the WGII and WGIII contributions, and the cross-working-group AR6 Synthesis Report (SYR).

IPCC 2021, Chap. 1

The structure of the AR6 WGI Report

Figure 1.1: The structure of the AR6 WGI Report. Shown are the three pillars of AR6 WGI, its relation to the WGII and WGIII contributions, and the cross-working-group AR6 Synthesis Report (SYR).

IPCC 2021, Chap. 1

Main relations between AR5 WGI and AR6 WGI chapters

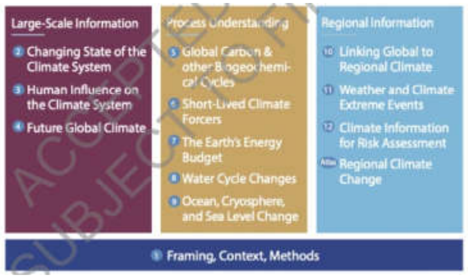

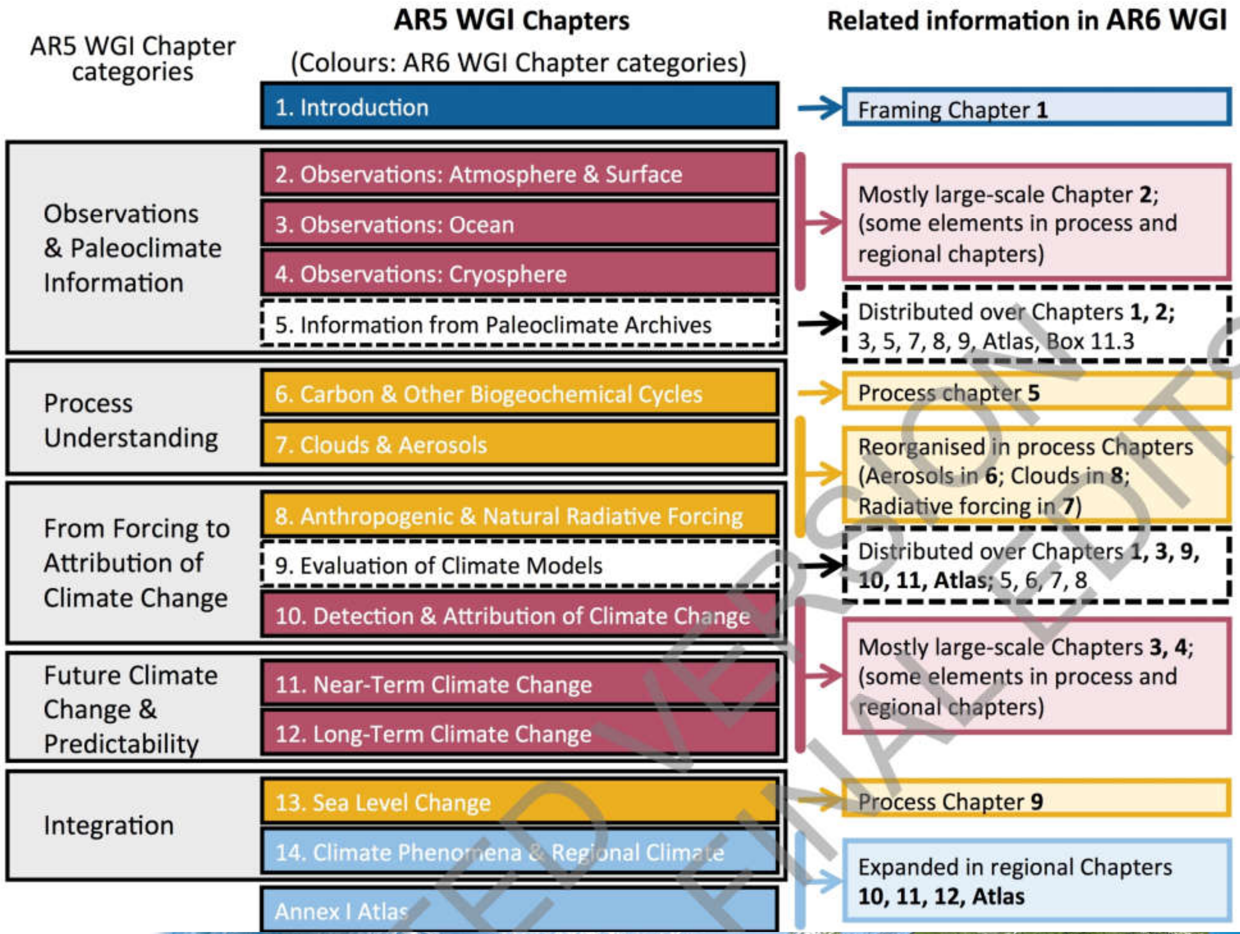

Figure 1.2: Main relations between AR5 WGI and AR6 WGI chapters. The left column shows the AR5 WGI chapter categories. The central column lists the AR5 WGI chapters, with the colour code indicating their relation to the AR6 WGI structure shown in Figure 1.1: Large-Scale Information (red), Process Understanding (gold), Regional Information (light blue), and Whole-Report Information (dark blue). AR5 WGI chapters depicted in white have their topics distributed over multiple AR6 WGI chapters and categories. The right column explains where to find related information in the AR6 WGI report.

IPCC 2021, Chap. 1

Statements in the Executive Summary

Framing and Context of the WGI Report (2)

Since the IPCC Fifth Assessment Report (AR5), the international policy context of IPCC reports has changed. The UN Framework Convention on Climate Change (UNFCCC, 1992) has the overarching objective of preventing ‘dangerous anthropogenic interference with the climate system’. Responding to that objective, the Paris Agreement (2015) established the long-term goals of ‘holding the increase in global average temperature to well below 2^{o}C above pre-industrial levels and pursuing efforts to limit the temperature increase to 1.5^{o}C above pre-industrial levels’ and of achieving ‘a balance between anthropogenic emissions by sources and removals by sinks of greenhouse gases in the second half of this century’. Parties to the Agreement have submitted Nationally Determined Contributions (NDCs) indicating their planned mitigation and adaptation strategies. However, the NDCs submitted as of 2020 are insufficient to reduce greenhouse gas emission enough to be consistent with trajectories limiting global warming to well below 2^{o}C above pre-industrial levels (*high confidence*). {1.1, 1.2}

IPCC 2021, Chap. 1

Characterizing understanding and uncertainty in assessment findings.

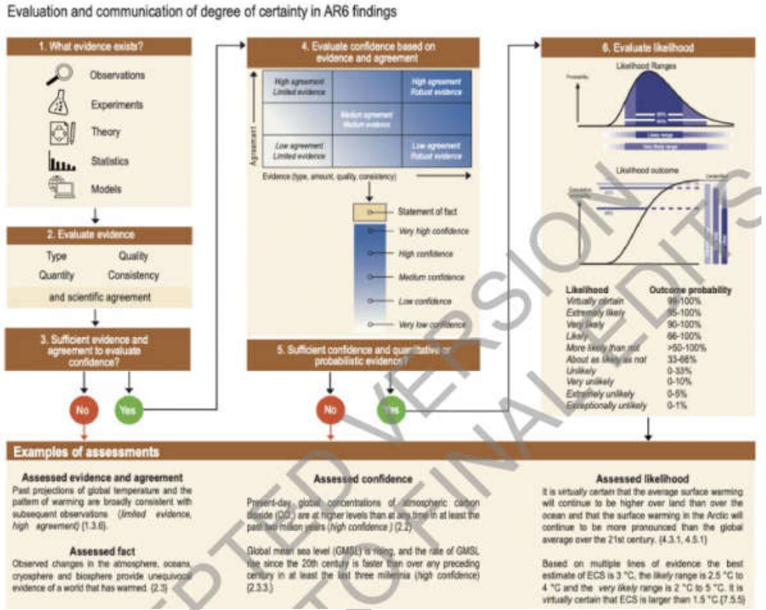

Box 1.1, Figure 1: The IPCC AR6 approach for characterizing understanding and uncertainty in assessment findings. This diagram illustrates the step-by-step process authors use to evaluate and communicate the state of knowledge in their assessment (Mastrandrea et al., 2010). Authors present evidence/agreement, confidence, or likelihood terms with assessment conclusions, communicating their expert judgments accordingly. Example conclusions drawn from this report are presented in the box at the bottom of the figure. [adapted from Mach et al. (2017)].

IPCC 2021, Chap. 1

Evaluation and communication of degree of certainty in AR6 findings

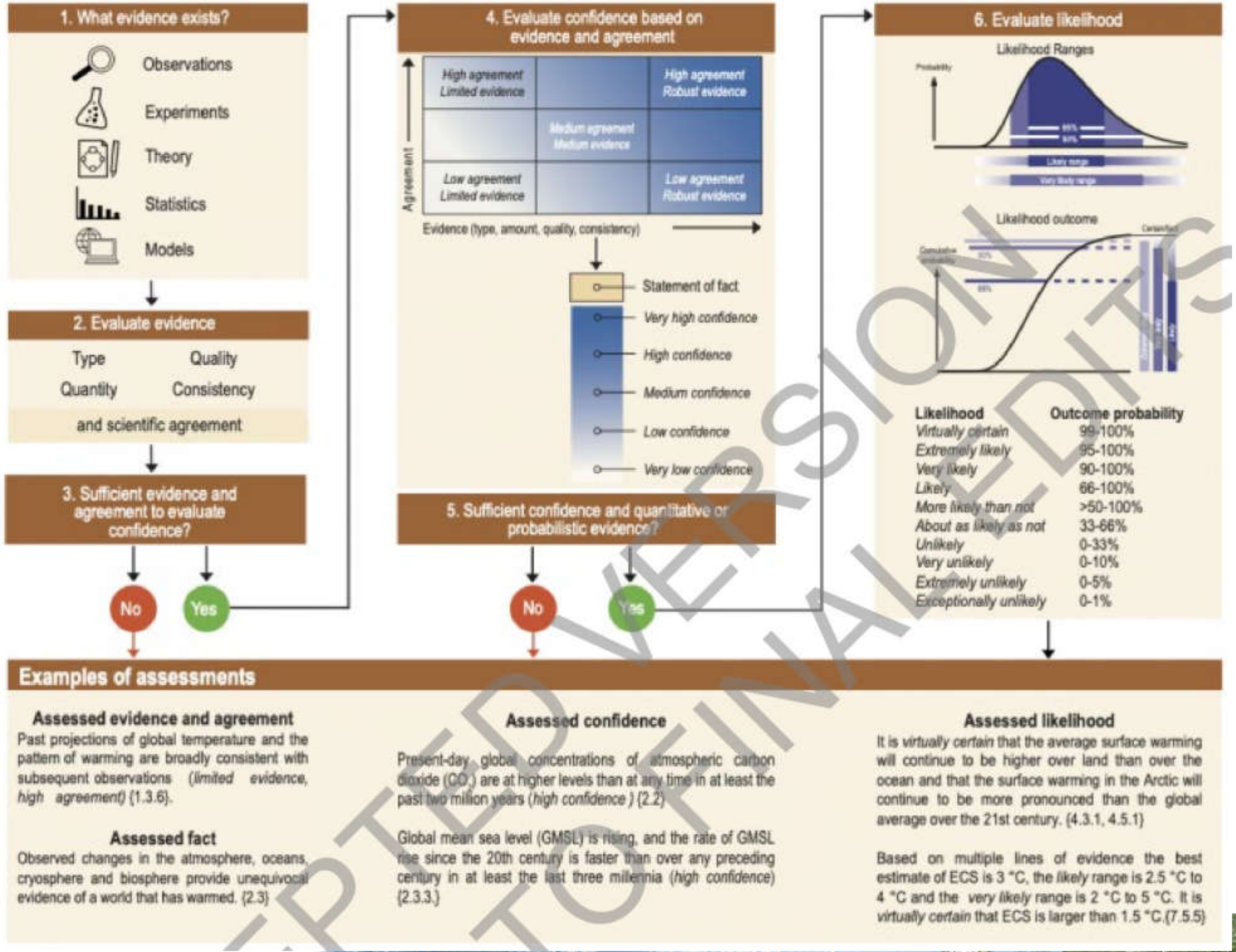

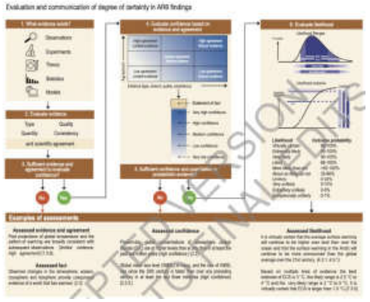

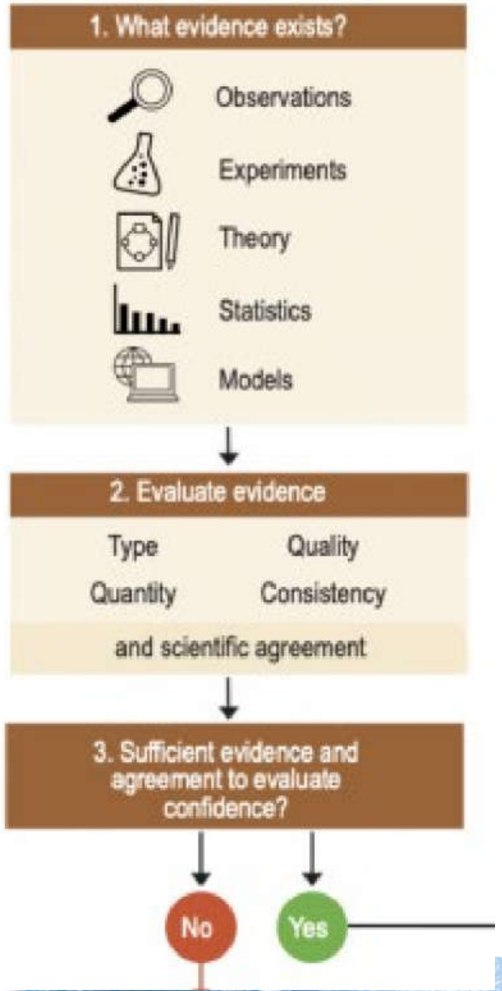
1. What evidence exists?
Observations
Experiments
Theory
Statistics
Models
2. Evaluate evidence
Type
Quality
Quantity
Consistency
and scientific agreement
3. Sufficient evidence and agreement to evaluate confidence?
No
Yes

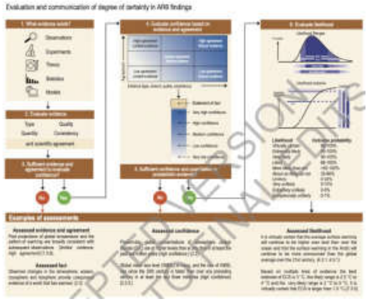

Examples of assessments

Assessed evidence and agreement

Past projections of global temperature and the pattern of warming are broadly consistent with subsequent observations (*limited evidence, high agreement*) {1.3.6}.

Assessed fact

Observed changes in the atmosphere, oceans, cryosphere and biosphere provide unequivocal evidence of a world that has warmed. {2.3}

Assessed confidence

Present-day global concentrations of atmospheric carbon dioxide (CO_2) are at higher levels than at any time in at least the past two million years (*high confidence*) {2.2}

Global mean sea level (GMSL) is rising, and the rate of GMSL rise since the 20th century is faster than over any preceding century in at least the last three millennia (*high confidence*) {2.3.3.}

Assessed likelihood

It is *virtually certain* that the average surface warming will continue to be higher over land than over the ocean and that the surface warming in the Arctic will continue to be more pronounced than the global average over the 21st century. {4.3.1, 4.5.1}

Based on multiple lines of evidence the best estimate of ECS is 3 °C, the *likely* range is 2.5 °C to 4 °C and the *very likely* range is 2 °C to 5 °C. It is *virtually certain* that ECS is larger than 1.5 °C.{7.5.5}

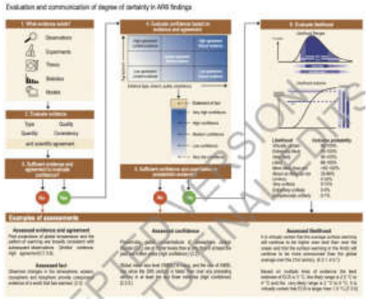

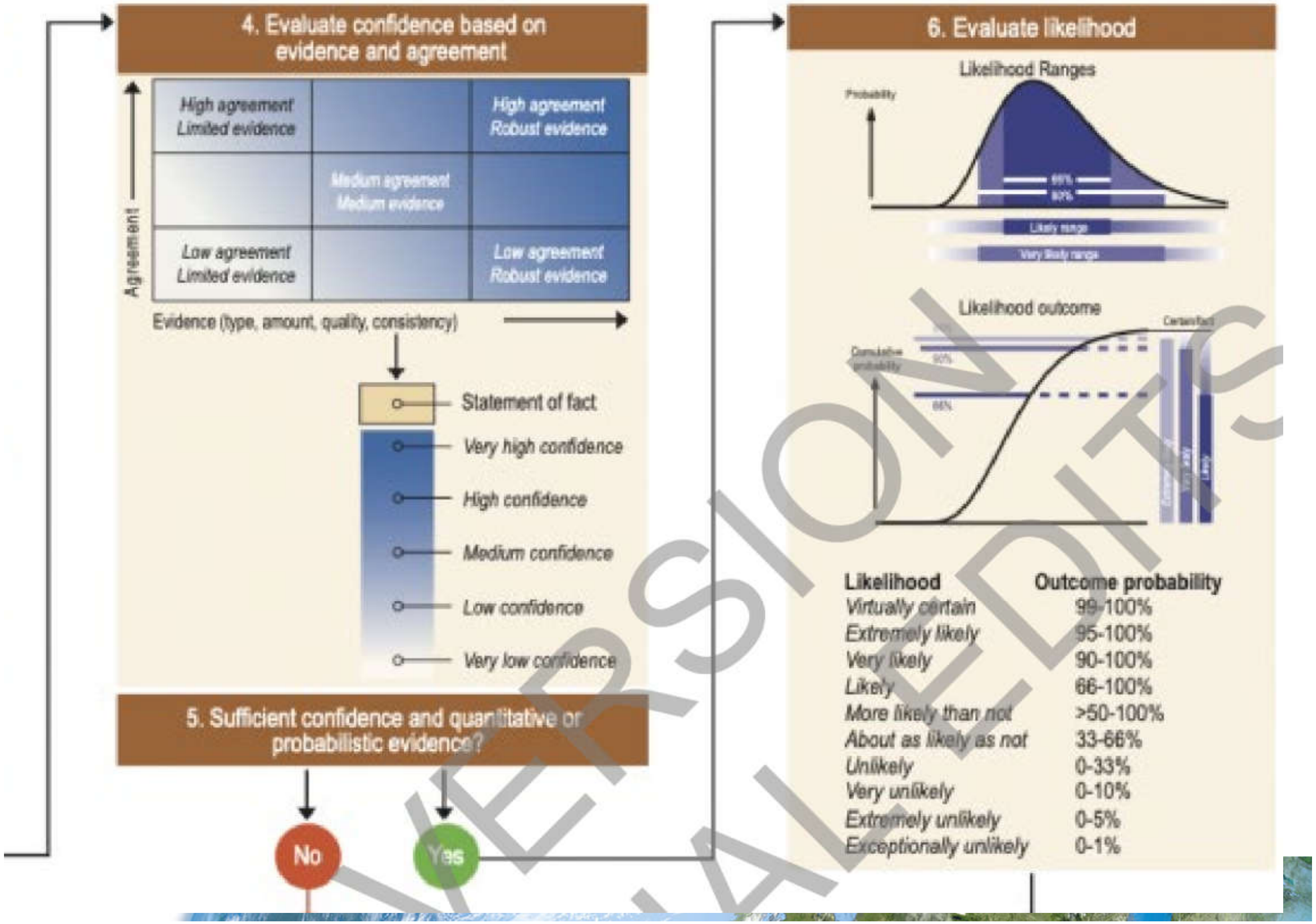

4. Evaluate confidence based on evidence and agreement
High agreement Limited evidence
High agreement Robust evidence
Medium agreement Medium evidence
Low agreement Limited evidence
Low agreement Robust evidence
Agreement
Evidence (type, amount, quality, consistency)
Statement of fact
Very high confidence
High confidence
Medium confidence
Low confidence
Very low confidence
5. Sufficient confidence and quantitative or probabilistic evidence?
No
Yes
6. Evaluate likelihood
Likelihood Ranges
Probability
66%
90%
Likely range
Very likely range
Likelihood outcome
Certain fact
Cumulative probability
90%
66%
Likely
Likelihood
Outcome probability
Virtually certain
99-100%
Extremely likely
95-100%
Very likely
90-100%
Likely
66-100%
More likely than not
>50-100%
About as likely as not
33-66%
Unlikely
0-33%
Very unlikely
0-10%
Extremely unlikely
0-5%
Exceptionally unlikely
0-1%

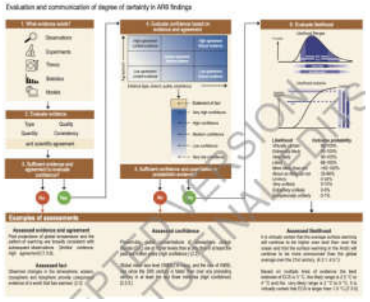

Examples of assessments

Assessed evidence and agreement

Past projections of global temperature and the pattern of warming are broadly consistent with subsequent observations (*limited evidence, high agreement*) {1.3.6}.

Assessed fact

Observed changes in the atmosphere, oceans, cryosphere and biosphere provide unequivocal evidence of a world that has warmed. {2.3}

Assessed confidence

Present-day global concentrations of atmospheric carbon dioxide (CO_2) are at higher levels than at any time in at least the past two million years (*high confidence*) {2.2}

Global mean sea level (GMSL) is rising, and the rate of GMSL rise since the 20th century is faster than over any preceding century in at least the last three millennia (*high confidence*) {2.3.3.}

Assessed likelihood

It is *virtually certain* that the average surface warming will continue to be higher over land than over the ocean and that the surface warming in the Arctic will continue to be more pronounced than the global average over the 21st century. {4.3.1, 4.5.1}

Based on multiple lines of evidence the best estimate of ECS is 3 °C, the *likely* range is 2.5 °C to 4 °C and the *very likely* range is 2 °C to 5 °C. It is *virtually certain* that ECS is larger than 1.5 °C.{7.5.5}

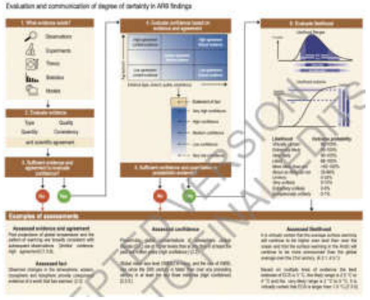

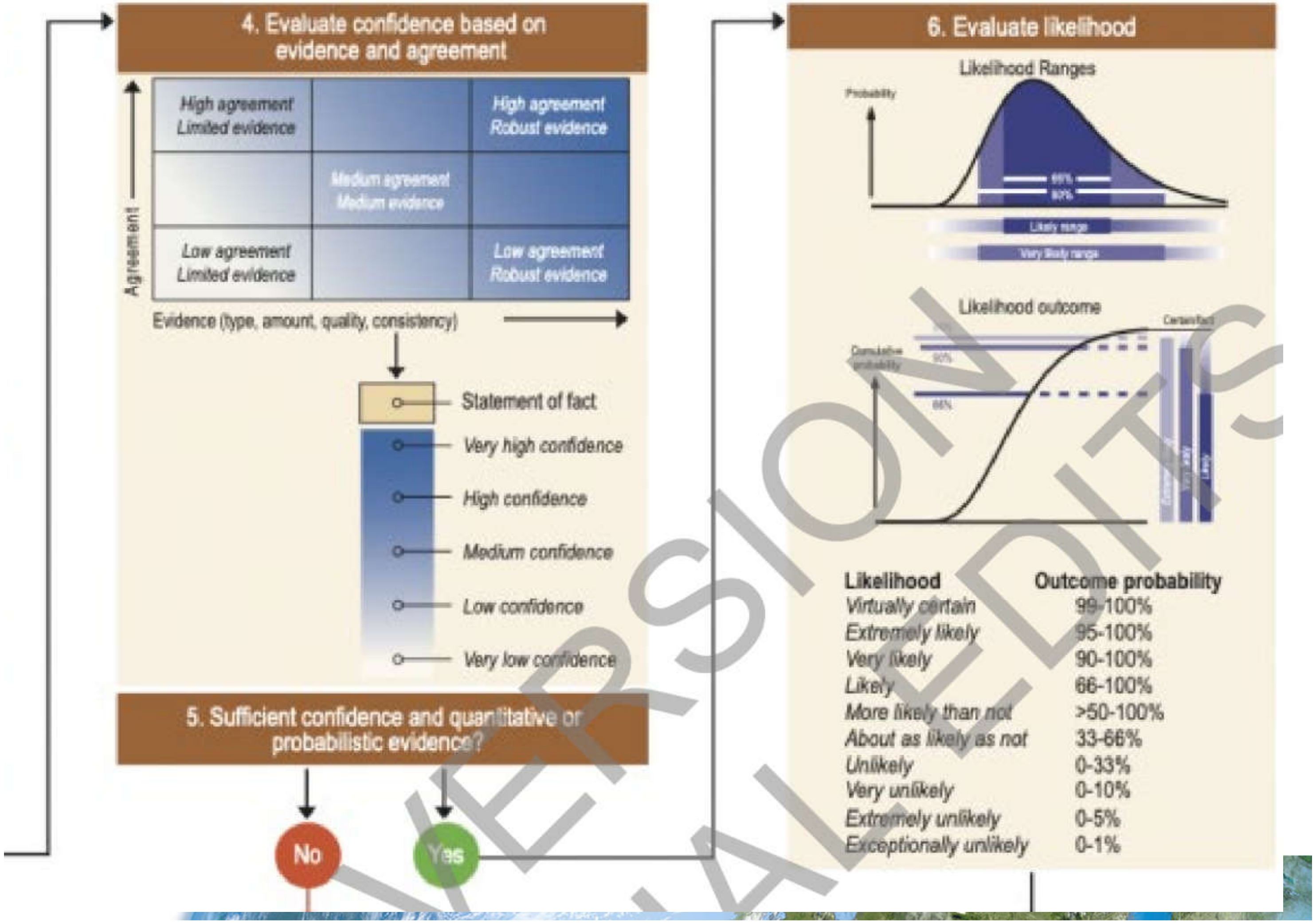
4. Evaluate confidence based on evidence and agreement
High agreement Limited evidence
High agreement Robust evidence
Medium agreement Medium evidence
Low agreement Limited evidence
Low agreement Robust evidence
Agreement
Evidence (type, amount, quality, consistency)
Statement of fact
Very high confidence
High confidence
Medium confidence
Low confidence
Very low confidence
5. Sufficient confidence and quantitative or probabilistic evidence?
No
Yes
6. Evaluate likelihood
Likelihood Ranges
Probability
66%
90%
Likely range
Very likely range
Likelihood outcome
Cumulative probability
Certain fact
Likelihood
Outcome probability
Virtually certain
99-100%
Extremely likely
95-100%
Very likely
90-100%
Likely
66-100%
More likely than not
>50-100%
About as likely as not
33-66%
Unlikely
0-33%
Very unlikely
0-10%
Extremely unlikely
0-5%
Exceptionally unlikely
0-1%

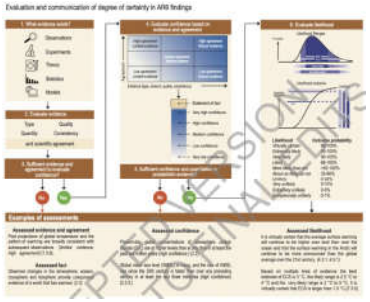

Examples of assessments

Assessed evidence and agreement

Past projections of global temperature and the pattern of warming are broadly consistent with subsequent observations (*limited evidence, high agreement*) {1.3.6}.

Assessed fact

Observed changes in the atmosphere, oceans, cryosphere and biosphere provide unequivocal evidence of a world that has warmed. {2.3}

Assessed confidence

Present-day global concentrations of atmospheric carbon dioxide (CO_2) are at higher levels than at any time in at least the past two million years (*high confidence*) {2.2}

Global mean sea level (GMSL) is rising, and the rate of GMSL rise since the 20th century is faster than over any preceding century in at least the last three millennia (*high confidence*) {2.3.3.}

Assessed likelihood

It is *virtually certain* that the average surface warming will continue to be higher over land than over the ocean and that the surface warming in the Arctic will continue to be more pronounced than the global average over the 21st century. {4.3.1, 4.5.1}

Based on multiple lines of evidence the best estimate of ECS is 3 °C, the *likely* range is 2.5 °C to 4 °C and the *very likely* range is 2 °C to 5 °C. It is *virtually certain* that ECS is larger than 1.5 °C.{7.5.5}

Statements in the Executive Summary

Framing and Context of the WGI Report (3)

This report provides information of potential relevance to the 2023 global stocktake. The 5-yearly stocktakes called for in the Paris Agreement will evaluate alignment among the Agreement's long-term goals, its means of implementation and support, and evolving global efforts in climate change mitigation (efforts to limit climate change) and adaptation (efforts to adapt to changes that cannot be avoided). In this context, WGI assesses, among other topics, remaining cumulative carbon emission budgets for a range of global warming levels, effects of long-lived and short-lived climate forcers, projected changes in sea level and extreme events, and attribution to anthropogenic climate change. {Cross-Chapter Box 1.1}

IPCC 2021, Chap. 1

Statements in the Executive Summary

Framing and Context of the WGI Report (4)

Understanding of the fundamental features of the climate system is robust and well established. Scientists in the 19th-century identified the major natural factors influencing the climate system. They also hypothesized the potential for anthropogenic climate change due to carbon dioxide (CO_2) emitted by fossil fuel combustion. The principal natural drivers of climate change, including changes in incoming solar volcanic activity, orbital cycles, and changes in global biogeochemical cycles, have been studied systematically since the early 20th century. Other major anthropogenic drivers, such as atmospheric aerosols (fine solid particles or liquid droplets), land-use change and non-CO_2 greenhouse gases, were identified by the 1970s. Since systematic scientific assessments began in the 1970s, the influence of human activity on the warming of the climate system has evolved from theory to established fact. Past projections of global surface temperature and the pattern of warming are broadly consistent with subsequent observations (*limited evidence, high agreement*), especially when accounting for the difference in radiative forcing scenarios used for making projections and the radiative forcings that actually occurred. {1.3.1 - 1.3.6}

IPCC 2021, Chap. 1

Climate science milestones between 1817-2021

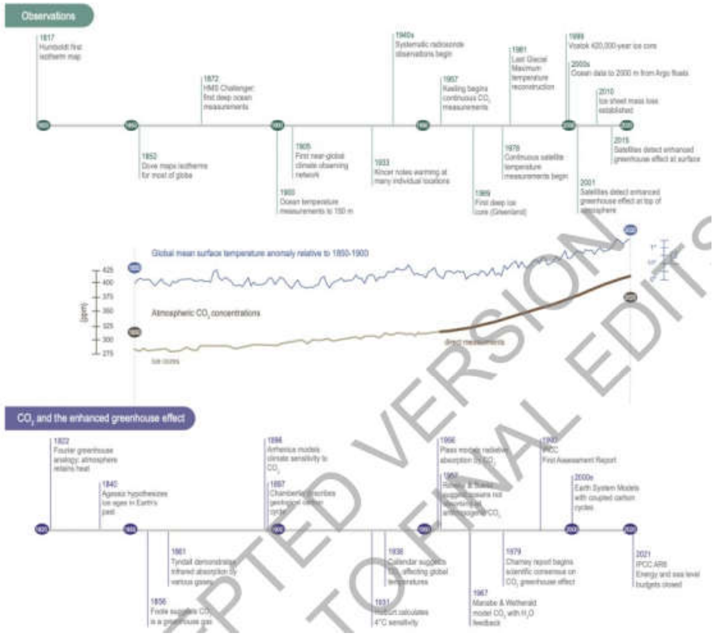

Figure 1.6: Climate science milestones, between 1817-2021. Milestones in observations (top); Curves of global surface air temperature (GMST) using HadCRUT5 (Morice et al., 2021) and atmospheric CO_2 concentrations from Antarctic ice cores (Lüthi et al., 2008; Bereiter et al., 2015) and direct air measurements from 1957 onwards (Tans and Keeling, 2020) (see Figure 1.4 for details) (middle). Milestone in scientific understanding of the CO2 enhanced greenhouse effect (bottom). Further details on each milestone are available in Chapter 1, Section 1.3, and Chapter 1 of AR4.

IPCC 2021, Chap. 1

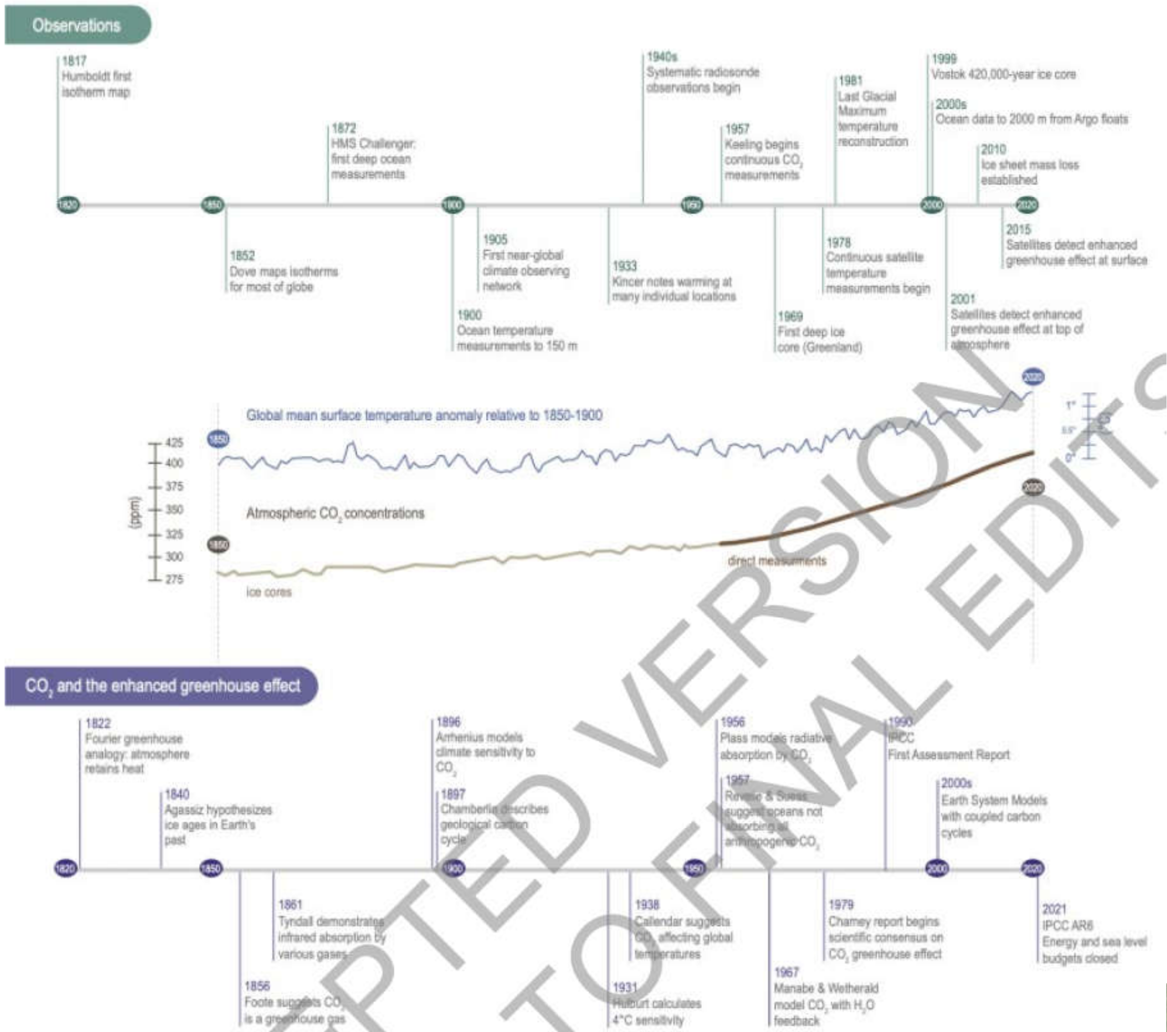

Observations
1817 Humboldt first isotherm map
1852 Dove maps isotherms for most of globe
1872 HMS Challenger: first deep ocean measurements
1900 Ocean temperature measurements to 150 m
1905 First near-global climate observing network
1933 Kincer notes warming at many individual locations
1940s Systematic radiosonde observations begin
1957 Keeling begins continuous CO_2 measurements
1969 First deep ice core (Greenland)
1978 Continuous satellite temperature measurements begin
1981 Last Glacial Maximum temperature reconstruction
1999 Vostok 420,000-year ice core
2000s Ocean data to 2000 m from Argo floats
2001 Satellites detect enhanced greenhouse effect at top of atmosphere
2010 Ice sheet mass loss established
2015 Satellites detect enhanced greenhouse effect at surface
1820
1850
1900
1950
2000
2020
Global mean surface temperature anomaly relative to 1850-1900
Atmospheric CO_2 concentrations
(ppm)
425
400
375
350
325
300
275
ice cores
direct measurements
1°
0.5°
0°
CO_2 and the enhanced greenhouse effect
1822 Fourier greenhouse analogy: atmosphere retains heat
1840 Agassiz hypothesizes ice ages in Earth's past
1856 Foote suggests CO_2 is a greenhouse gas
1861 Tyndall demonstrates infrared absorption by various gases
1896 Arrhenius models climate sensitivity to CO_2
1897 Chamberlin describes geological carbon cycle
1931 Hulburt calculates 4°C sensitivity
1938 Callendar suggests CO_2 affecting global temperatures
1956 Plass models radiative absorption by CO_2
1957 Revelle & Suess suggest oceans not absorbing all anthropogenic CO_2
1967 Manabe & Wetherald model CO_2 with H_2O feedback
1979 Charney report begins scientific consensus on CO_2 greenhouse effect
1990 IPCC First Assessment Report
2000s Earth System Models with coupled carbon cycles
2021 IPCC AR6 Energy and sea level budgets closed

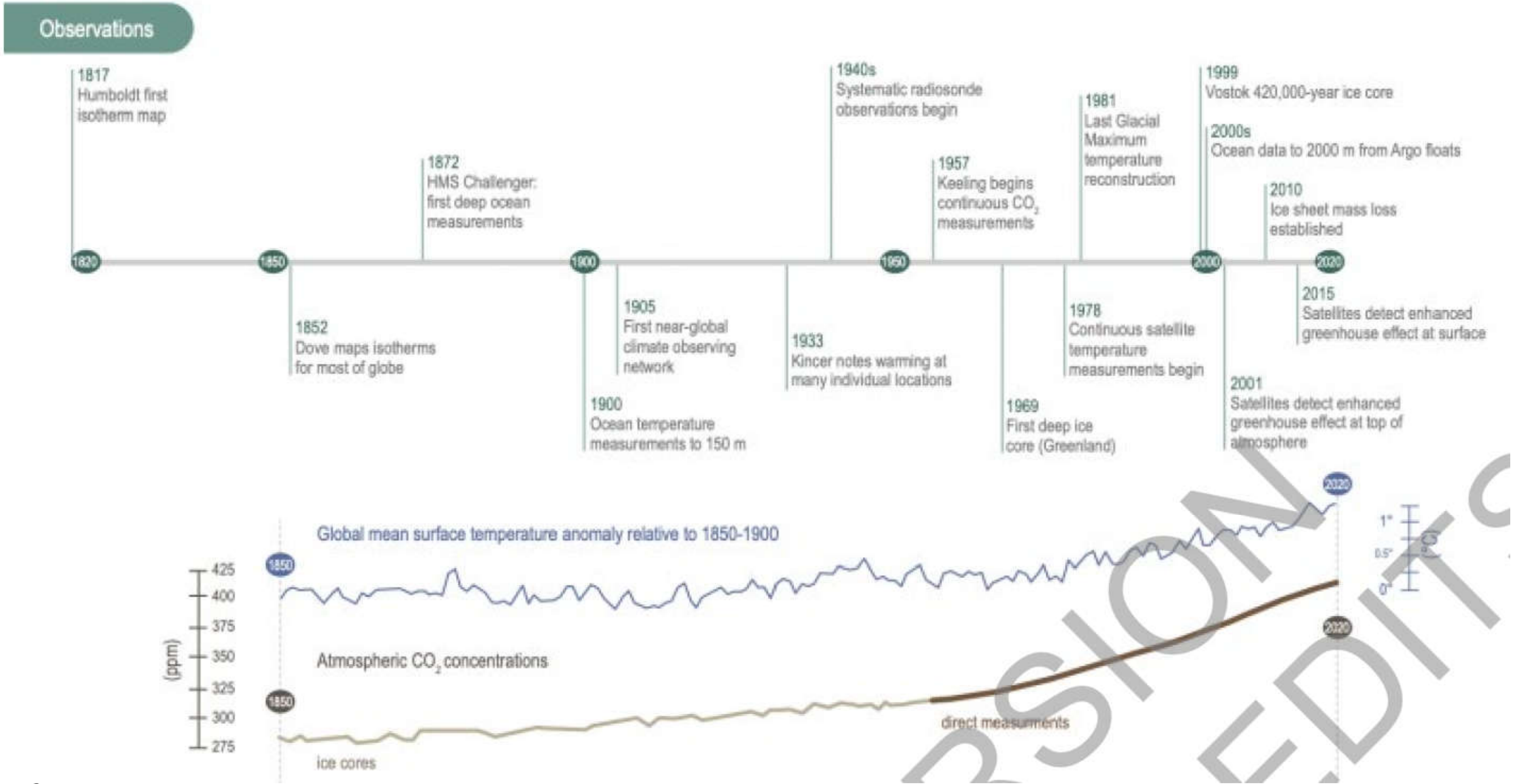

Observations
1817
Humboldt first isotherm map
1852
Dove maps isotherms for most of globe
1872
HMS Challenger: first deep ocean measurements
1900
Ocean temperature measurements to 150 m
1905
First near-global climate observing network
1933
Kincer notes warming at many individual locations
1940s
Systematic radiosonde observations begin
1957
Keeling begins continuous CO_2 measurements
1969
First deep ice core (Greenland)
1978
Continuous satellite temperature measurements begin
1981
Last Glacial Maximum temperature reconstruction
1999
Vostok 420,000-year ice core
2000s
Ocean data to 2000 m from Argo floats
2001
Satellites detect enhanced greenhouse effect at top of atmosphere
2010
Ice sheet mass loss established
2015
Satellites detect enhanced greenhouse effect at surface
1820
1850
1900
1950
2000
2020
Global mean surface temperature anomaly relative to 1850-1900
1°
0.5°
0°
°C
Atmospheric CO_2 concentrations
(ppm)
425
400
375
350
325
300
275
ice cores
direct measurements

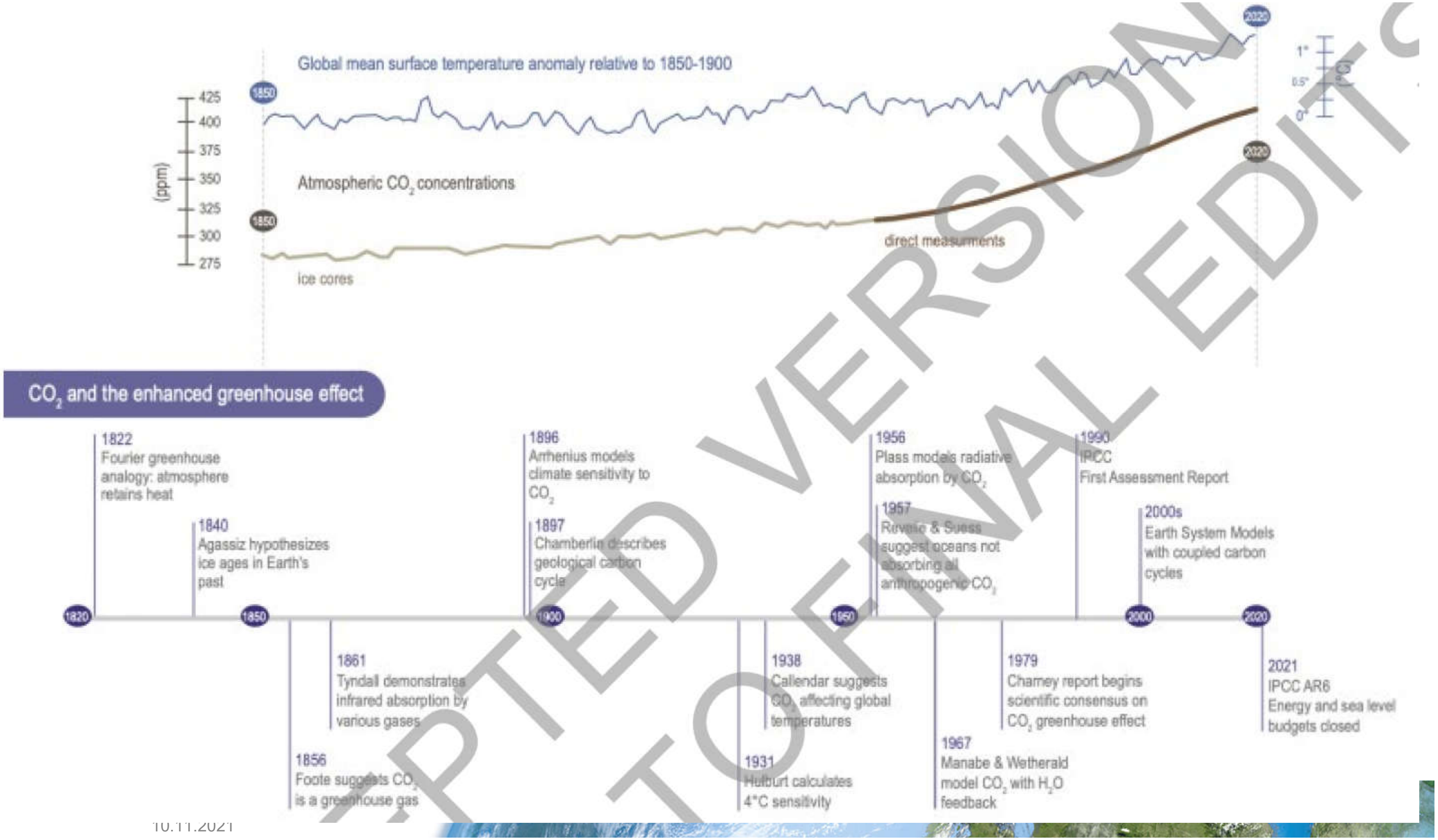

Global mean surface temperature anomaly relative to 1850-1900
Atmospheric CO2 concentrations
(ppm)
425
400
375
350
325
300
275
1850
2020
1°
0.5°
0°
(°C)
direct measurements
ice cores
CO2 and the enhanced greenhouse effect
1822 Fourier greenhouse analogy: atmosphere retains heat
1840 Agassiz hypothesizes ice ages in Earth's past
1896 Arrhenius models climate sensitivity to CO2
1897 Chamberlin describes geological carbon cycle
1956 Plass models radiative absorption by CO2
1957 Revelle & Suess suggest oceans not absorbing all anthropogenic CO2
1990 IPCC First Assessment Report
2000s Earth System Models with coupled carbon cycles
1820
1850
1900
1950
2000
2020
1856 Foote suggests CO2 is a greenhouse gas
1861 Tyndall demonstrates infrared absorption by various gases
1931 Hulburt calculates 4°C sensitivity
1938 Callendar suggests CO2 affecting global temperatures
1967 Manabe & Wetherald model CO2 with H2O feedback
1979 Charney report begins scientific consensus on CO2 greenhouse effect
2021 IPCC AR6 Energy and sea level budgets closed

Statements in the Executive Summary

Framing and Context of the WGI Report (5)

Global surface temperatures increased by about 0.1°C (*likely* range –0.1°C to +0.3°C, *medium confidence*) between the period around 1750 and the 1850–1900 period, with anthropogenic factors responsible for a warming of 0.0°C – 0.2°C (*likely range, medium confidence*). This assessed change in temperature before 1850–1900 is not included in the AR6 assessment of global warming to date, to ensure consistency with previous IPCC assessment reports, and because of the lower confidence in the estimate. There was *likely* a net anthropogenic forcing of 0.0 – 0.3 Wm^{-2} in 1850–1900 relative to 1750 (*medium confidence*), with radiative forcing from increases in atmospheric greenhouse gas concentrations being partially offset by anthropogenic aerosol emissions and land-use change. Net radiative forcing from solar and volcanic activity is estimated to be smaller than ±0.1 Wm^{-2} for the same period. {Cross Chapter Box 1.2, 1.4.1, Cross Chapter Box 2.3}

IPCC 2021, Chap. 1

Changes are occurring throughout the climate system

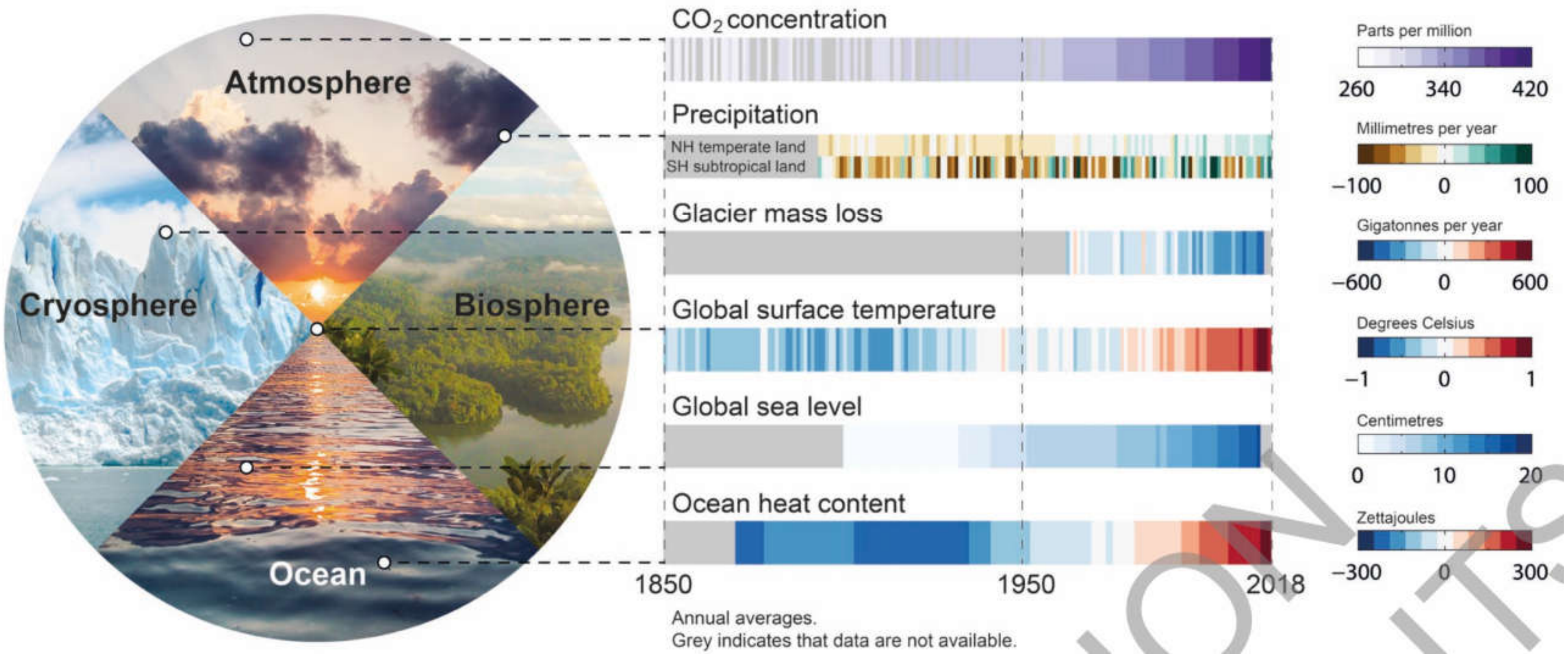

Figure 1.4: Changes are occurring throughout the climate system. Left: Main realms of the climate system:

Figure 1.4: Changes are occurring throughout the climate system. Left: Main realms of the climate system: atmosphere, biosphere, cryosphere, and ocean. Right: Six key indicators of ongoing changes since 1850, or the start of the observational or assessed record, through 2018. Each stripe indicates the global (except for precipitation which shows two latitude band means), annual mean anomaly for a single year, relative to a multi-year baseline (except for CO_2 concentration and glacier mass loss, which are absolute values). Grey indicates that data are not available. Datasets and baselines used are: (1) CO_2: Antarctic ice cores (Lüthi et al., 2008; Bereiter et al., 2015) and direct air measurements (Tans and Keeling, 2020) (see Figure 1.5 for details); (2) precipitation: Global Precipitation Climatology Centre (GPCC) V8 (updated from Becker et al. 2013), baseline 1961-1990 using land areas only with latitude bands 33°N–66°N and 15°S–30°S; (3) glacier mass loss: Zemp et al., 2019; (4) global surface air temperature (GMST): HadCRUT5 (Morice et al., 2021), baseline 1961–1990; (5) sea level change: (Dangendorf et al., 2019), baseline 1900–1929; (6) ocean heat content (model-observation hybrid): Zanna et al., (2019), baseline 1961–1990. Further details on data sources and processing are available in the chapter data table (Table

IPCC 2021, Chap. 1

Jahresmittel der Temperatur am Hohenpeißenberg (seit 1781)

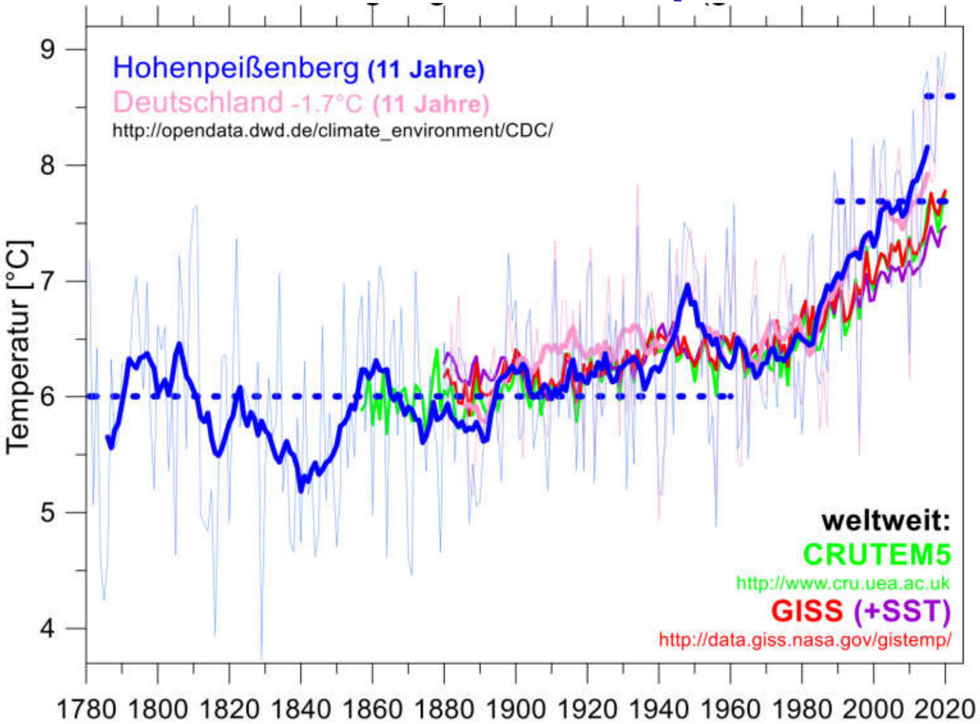

***Abbildung 1:** Jahresmittel der Temperatur am Hohenpeißenberg (blaue Kurven), sowie über Deutschland (rosa Kurven, um 1.7°C nach unten verschoben). Dünne Linien: Jahresmittel. Dicke Linien: gleitendes Mittel über 11 Jahre. Dicke gestrichelte Linien: langjährige Hohenpeißenberger Mittel der Jahre 1781 bis 1960 (6°C), 1990 bis 2020 (7.7°C) und 2015 bis 2020 (8.6°C). Zum Vergleich sind auch weltweite Temperaturanomalien der Landoberfläche gezeigt (CRUTEM5 und GISS, 6.45°C nach oben verschoben). GISS liefert zusätzlich die weltweite Land- und Meeresoberflächen Temperaturanomalie (+SST). Weitere Informationen siehe angegebene Webseiten, sowie DWD Mitteilung vom Januar 2020.*

ca. 1900

~ heute

GAW Brief des DWD Nr. 80, 2021

wikipedia

Wetterbeobachtung im Stift Kremsmünster (Österreich), seit 1762

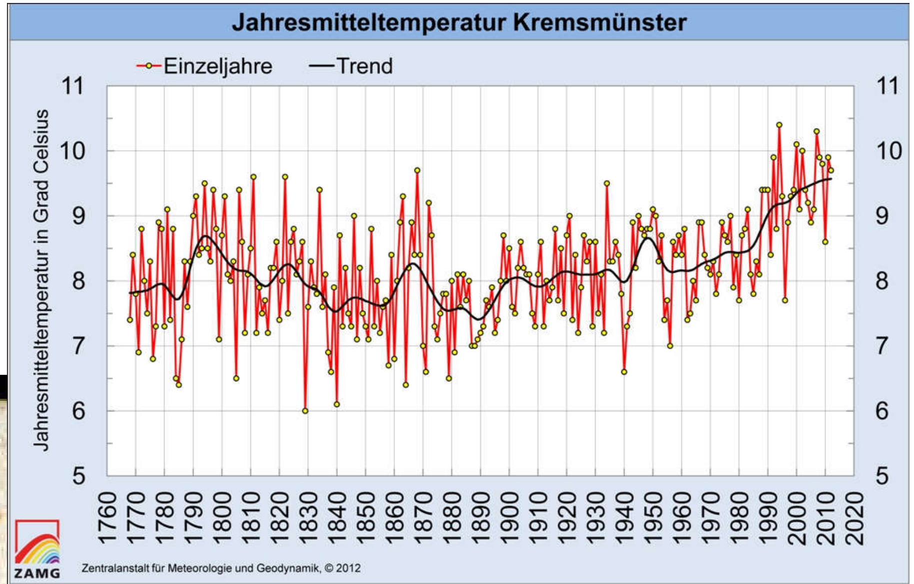

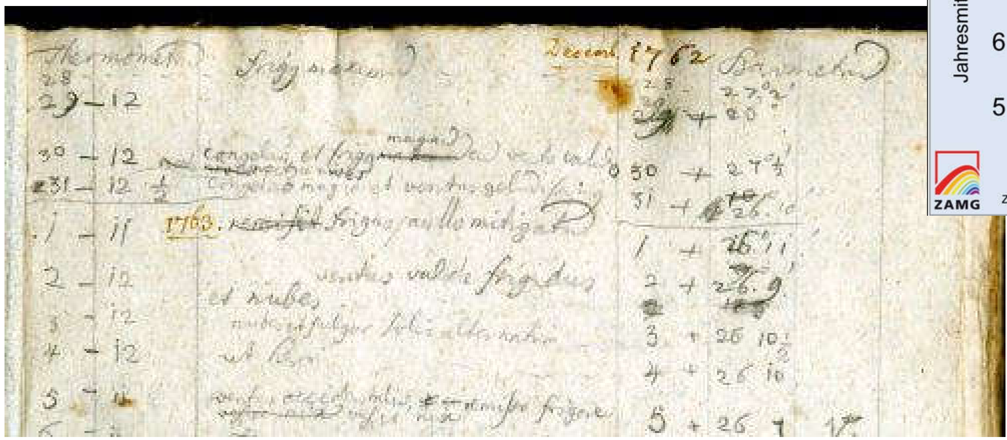

www.zamg.ac.at

"28. December 1762, frigus maximus, Barometer 27° 2´ "

Long-term context of anthropogenic climate change

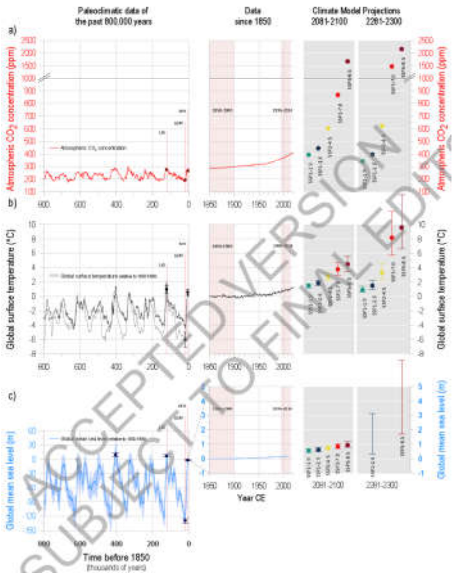

IPCC 2021, Chap. 1

Figure 1.5: Long-term context of anthropogenic climate change based on selected paleoclimatic reconstructions over the past 800,000 years for three key indicators: atmospheric CO_2 concentrations, Global Mean Surface Temperature (GMST), and Global Mean Sea Level (GMSL). a) Measurements of CO_2 in air enclosed in Antarctic ice cores (Lüthi et al., 2008; Bereiter et al., 2015 [a compilation]; uncertainty ±1.3ppm; see Chapter 2, Section 2.2.3 and Chapter 5, Section 5.1.2 for an assessment) and direct air measurements (Tans and Keeling, 2020; uncertainty ±0.12 ppm). Projected CO_2 concentrations for five Shared Socioeconomic Pathways (SSP) scenarios are indicated by dots on the right-hand side panels of the figure (grey background) (Meinshausen et al., 2020; SSPs are described in Section 1.6). b) Reconstruction of GMST from marine paleoclimate proxies (light grey: Snyder (2016); dark grey: Hansen et al. (2013); see Chapter 2, Section 2.3.1 for an assessment). Observed and reconstructed temperature changes since 1850 are the AR6 assessed mean (referenced to 1850–1900; Box TS.3; 2.3.1.1); dots/whiskers on the right-hand side panels of the figure (grey background) indicate the projected mean and ranges of warming derived from Coupled Model Intercomparison Project Phase 6 (CMIP6) SSP-based (2081–2100) and Model for the Assessment of Greenhouse Gas Induced Climate Change (MAGICC7) (2300) simulations (Chapter 4, Tables 4.5 and 4.9). c) Sea level changes reconstructed from a stack of oxygen isotope measurements on seven ocean sediment cores (Spratt and Lisiecki, 2016; see Chapter 2, Section 2.3.3.3 and Chapter 9, Section 9.6.2 for an assessment). The sea level record from 1850 to 1900 is from Kopp et al. (2016), while the 20th century record is an updated ensemble estimate of GMSL change (Palmer et al., 2021; see also Chapter 2, Section 2.3.3.3 and Chapter 9, Section 9.6.1.1). Dots/whiskers on the right-hand side panels of the figure (grey background) indicate the projected median and ranges derived from SSP-based simulations (2081–2100: Chapter 9, Table 9.9; 2300: Chapter 9, Section 9.6.3.5). Best estimates (dots) and uncertainties (whiskers) as assessed by Chapter 2 are included in the left and middle panels for each of the three indicators and selected paleo-reference periods used in this report (CO_2: Chapter 2, Table 2.1; GMST: Chapter 2, Section 2.3.1.1 and Cross-Chapter Box 2.3, Table 1 in Chapter 2; GMSL: Chapter 2, Section 2.3.3.3 and Chapter 9, Section 9.6.2. See also Cross-Chapter Box 2.1 in Chapter 2). Selected paleo-reference periods: LIG – Last Interglacial; LGM – Last Glacial Maximum; MH – mid-Holocene (Cross-Chapter Box 2.1, Table 1 in Chapter 2). The non-labelled best estimate in panel c) corresponds to the sea level high-stand during Marine Isotope Stage 11, about 410,000 years ago (see Chapter 9, Section 9.6.2). Further details on data sources and processing are available in the chapter data table (Table 1.SM.1).

Long-term context of anthropogenic climate change

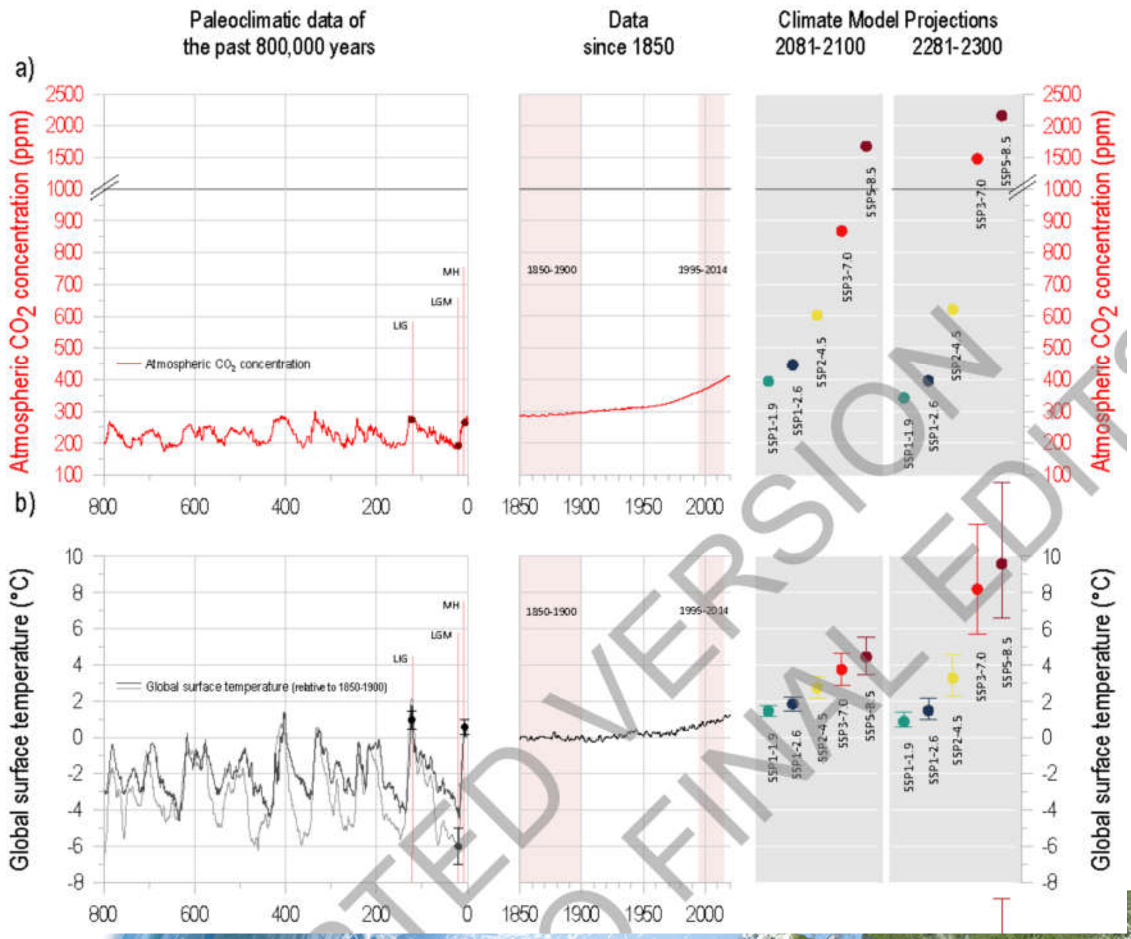

IPCC 2021, Chap. 1

Long-term context of anthropogenic climate change

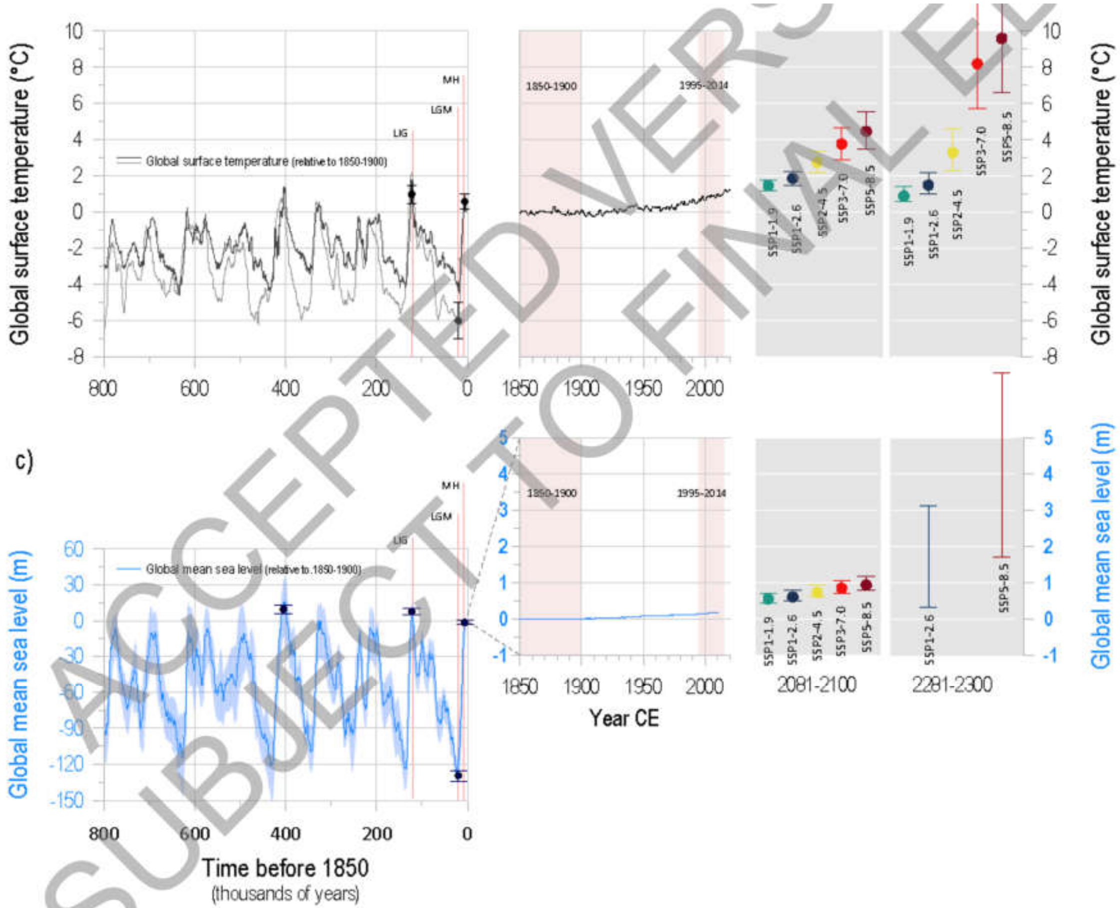

IPCC 2021, Chap. 1

Callendar's estimates of global land temperature variations and their possible causes.

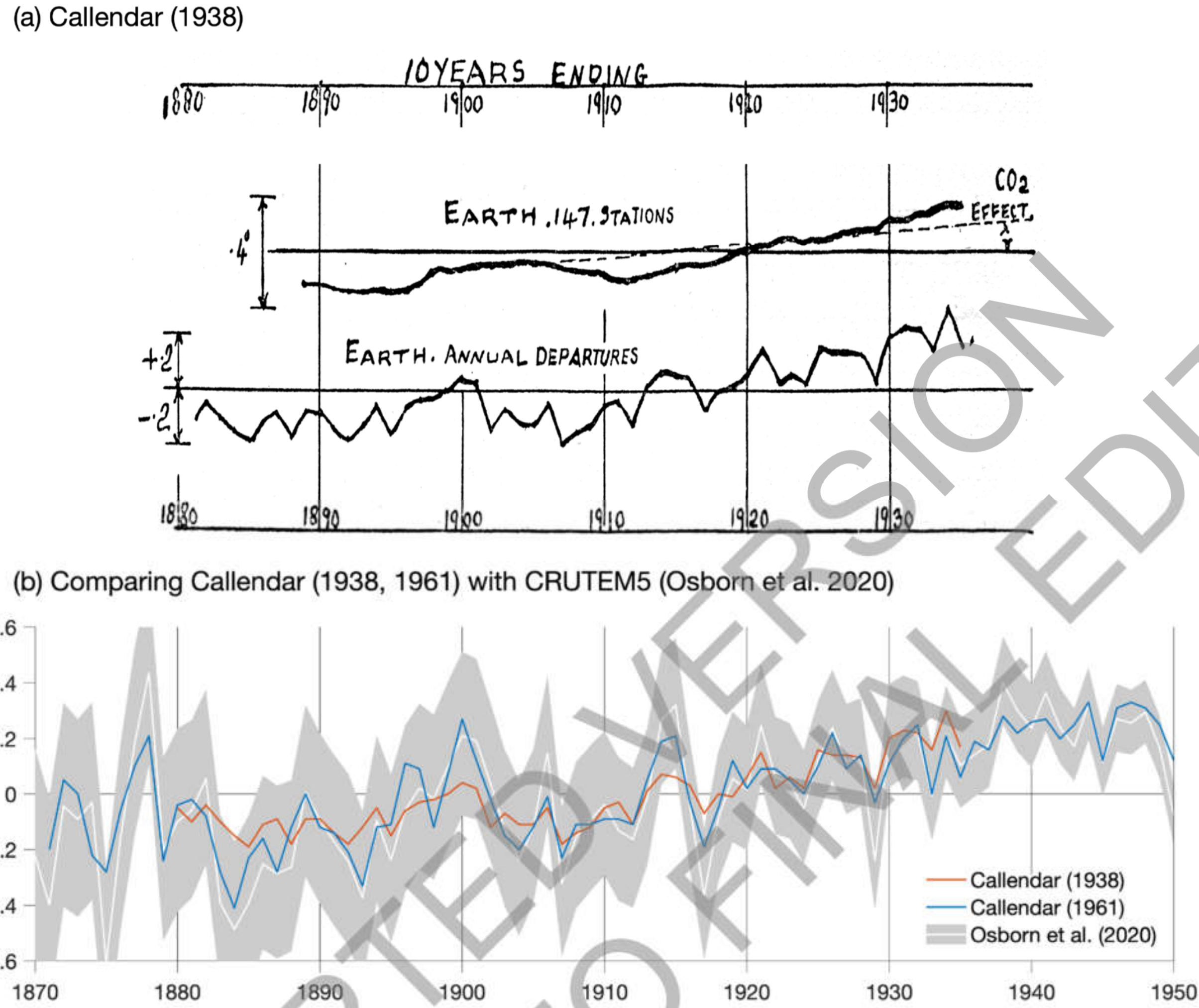

Figure 1.8: G.S. Callendar's estimates of global land temperature variations and their possible causes. (a) The original figure from Callendar (1938), using measurements from 147 surface stations for 1880–1935, showing: (top) ten-year moving departures from the mean of 1901-1930 (°C), with the dashed line representing his estimate of the 'CO_2 effect' on temperature rise, and (bottom) annual departures from the 1901–1930 mean (°C). (b) Comparing the estimates of global land (60°S–60°N) temperatures tabulated in Callendar (1938, 1961) with a modern reconstruction (Osborn et al., 2021) for the same period, after (Hawkins and Jones (2013). Further details on data sources and processing are available in the chapter data table (Table 1.SM.1).

IPCC 2021, Chap. 1

Range of projected temperature change for 1990–2030 for various regions defined in IPCC First Assessment Report (FAR)

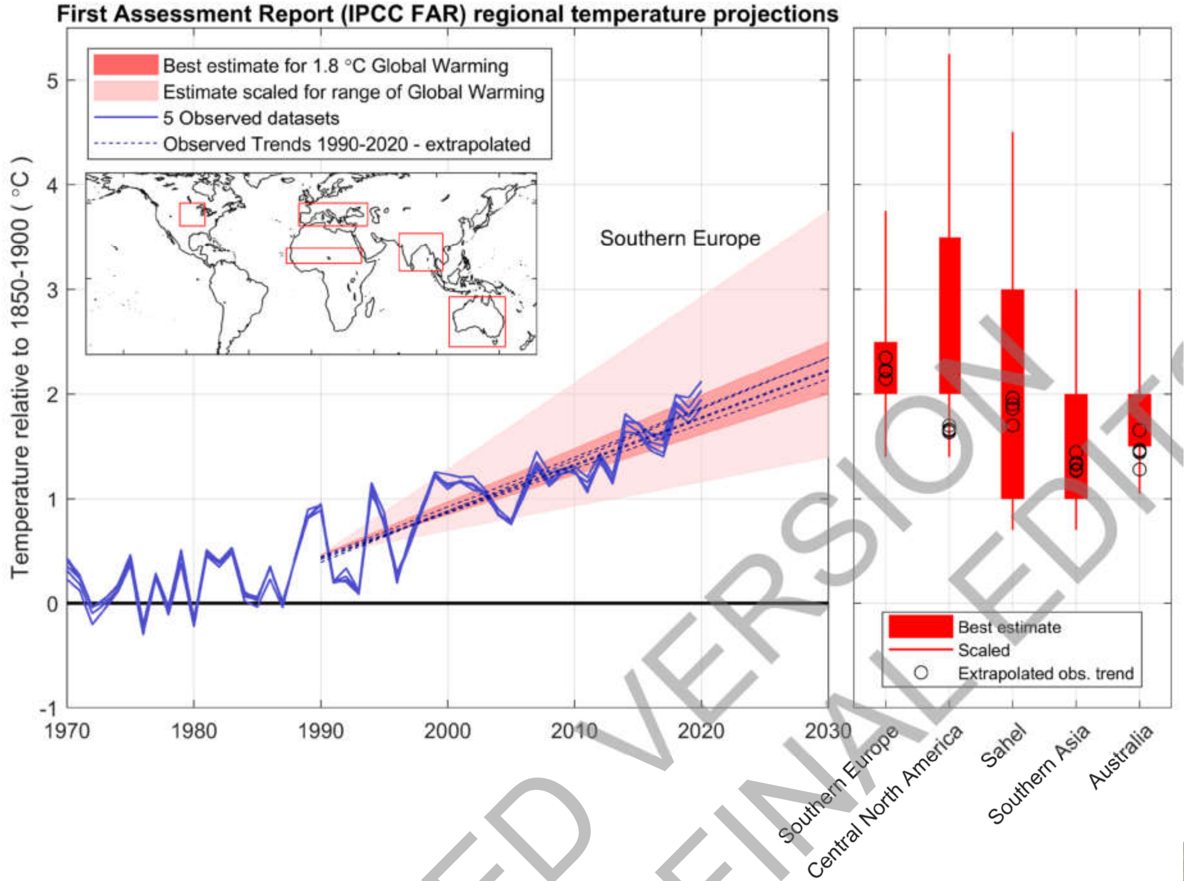

Figure 1.10: Range of projected temperature change for 1990–2030 for various regions defined in IPCC First Assessment Report (FAR). The left panel shows the FAR projections (IPCC, 1990) for Southern Europe, with darker red bands representing the range of projected change given for the best estimate of 1.8°C global warming since pre-industrial to 2030, and the fainter red bands show the range scaled by –30% to +50% for lower and higher estimates of global warming. Blue lines show the regionally averaged observations from several global temperature gridded datasets, and blue dashed lines show the linear trends in those datasets for 1990–2020 extrapolated to 2030. Observed datasets are: HadCRUT5, Cowtan and Way, GISTEMP, Berkeley Earth and NOAA GlobalTemp. The inset map shows the definition of the FAR regions used. The right panel shows projected temperature changes by 2030 for the various FAR regions, compared to the extrapolated observational trends, following Grose et al. (2017). Further details on data sources and processing are available in the chapter data table (Table 1.SM.1).

IPCC 2021, Chap. 1

Changes in radiative forcing from 1750 to 2019

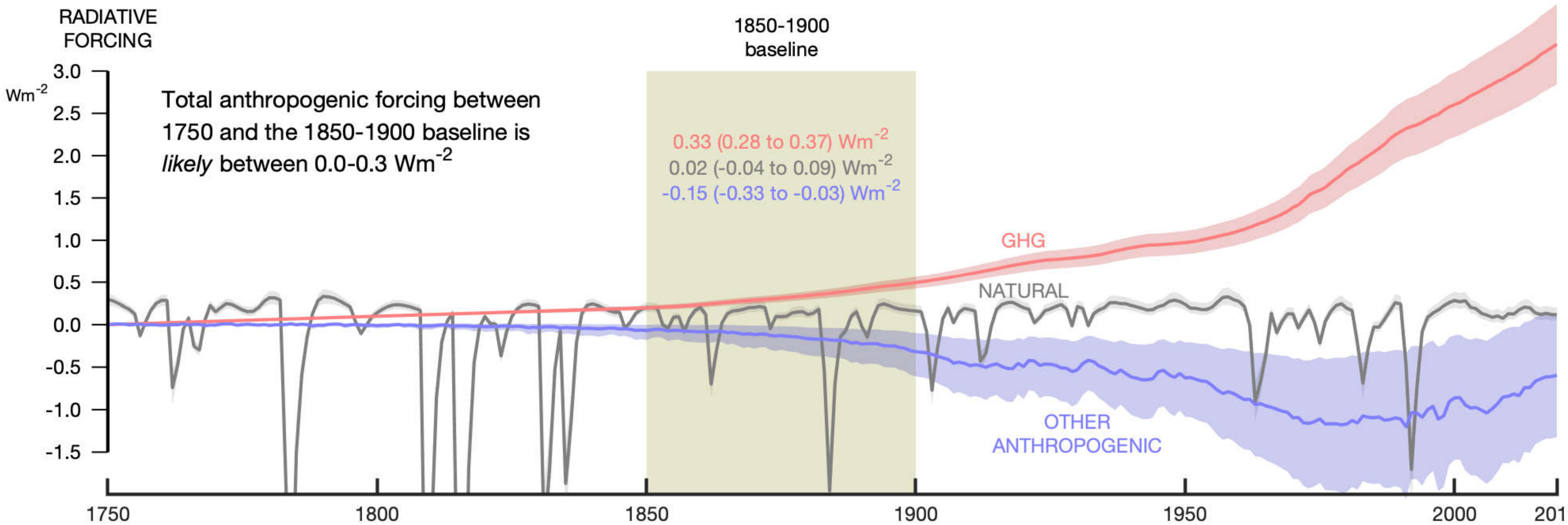

Cross-Chapter Box 1.2, Figure 1: Changes in radiative forcing from 1750 to 2019. The radiative forcing estimates from the AR6 emulator (see Cross-Chapter Box 7.1 in Chapter 7) are split into GHG, other anthropogenic (mainly aerosols and land use) and natural forcings, with the average over the 1850–1900 baseline shown for each. Further details on data sources and processing are available in the chapter data table (Table 1.SM.1).

IPCC 2021, Chap. 1

Statements in the Executive Summary

Framing and Context of the WGI Report (6)

Natural climate variability can temporarily obscure or intensify anthropogenic climate change on decadal time scales, especially in regions with large internal interannual-to-decadal variability. At the current level of global warming, an observed signal of temperature change relative to the 1850–1900 baseline has emerged above the levels of background variability over virtually all land regions (*high confidence*). Both the rate of long-term change and the amplitude of interannual (year-to-year) variability differ from global to regional to local scales, between regions and across climate variables, thus influencing when changes become apparent. Tropical regions have experienced less warming than most others, but also exhibit smaller interannual variations in temperature. Accordingly, the signal of change is more apparent in tropical regions than in regions with greater warming but larger interannual variations (*high confidence*). {1.4.2, FAQ1.2}

IPCC 2021, Chap. 1

IPCC 2021, Chap. 1

Simulated changes in various climate indicators under historical and RCP4.5 scenarios using the MPI ESM Grand Ensemble

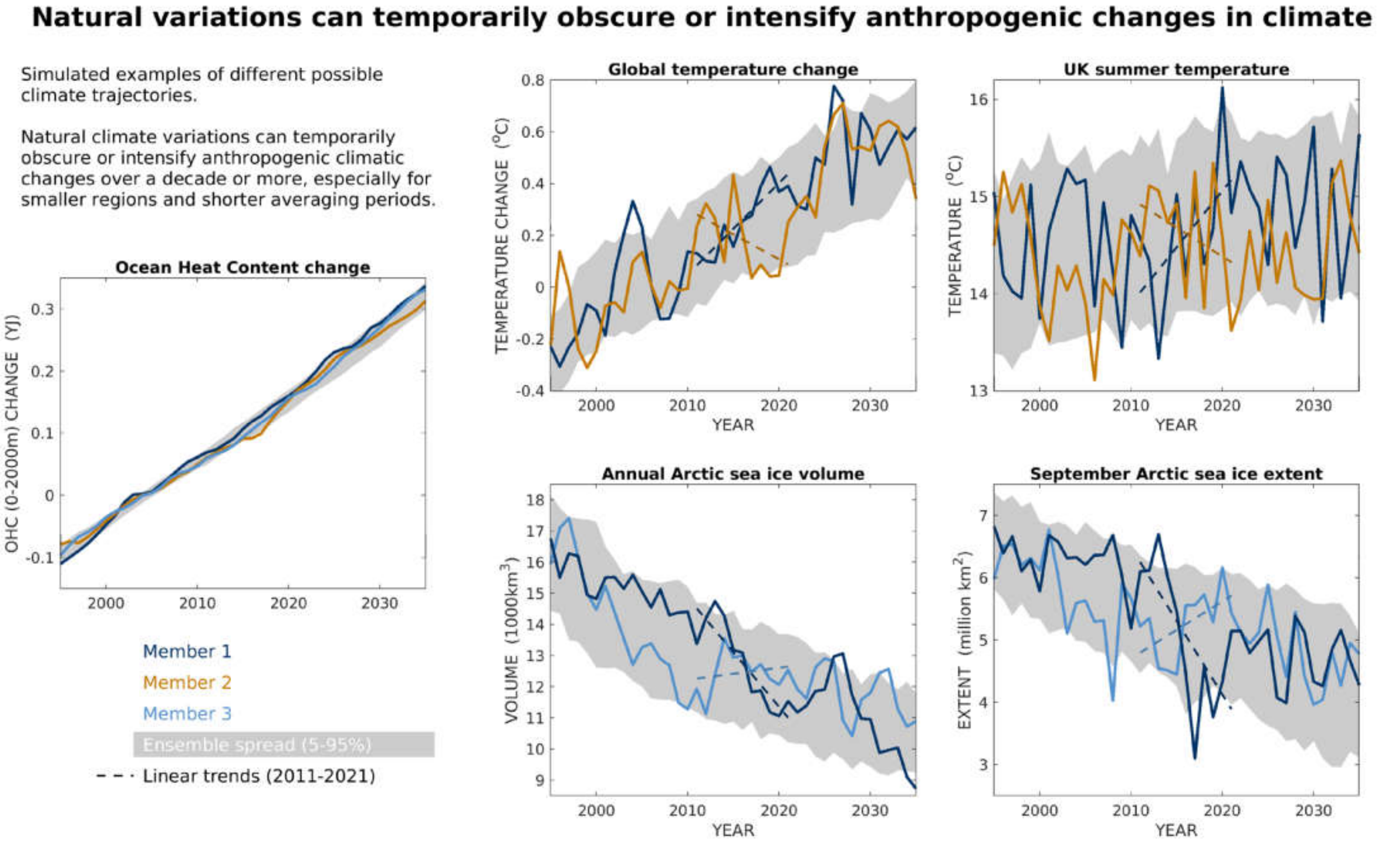

Figure 1.13: Simulated changes in various climate indicators under historical and RCP4.5 scenarios using the MPI ESM Grand Ensemble. The grey shading shows the 5–95% range from the 100-member ensemble. The coloured lines represent individual example ensemble members, with linear trends for the 2011–2021 period indicated by the thin dashed lines. Changes in Ocean Heat Content (OHC) over the top 2000m represents the integrated signal of global warming (left). The top row shows surface air temperature-related indicators (annual GSAT change and UK summer temperatures) and the bottom row shows Arctic sea-ice related indicators (annual ice volume and September sea ice extent). For smaller regions and for shorter time period averages the variability increases and simulated short-term trends can temporarily obscure or intensify anthropogenic changes in climate. Data from Maher et al., (2019). Further details on data sources and processing are available in the chapter data table (Table 1.SM.1).

IPCC 2021, Chap. 1

Changes in tropopause height and surface temperature

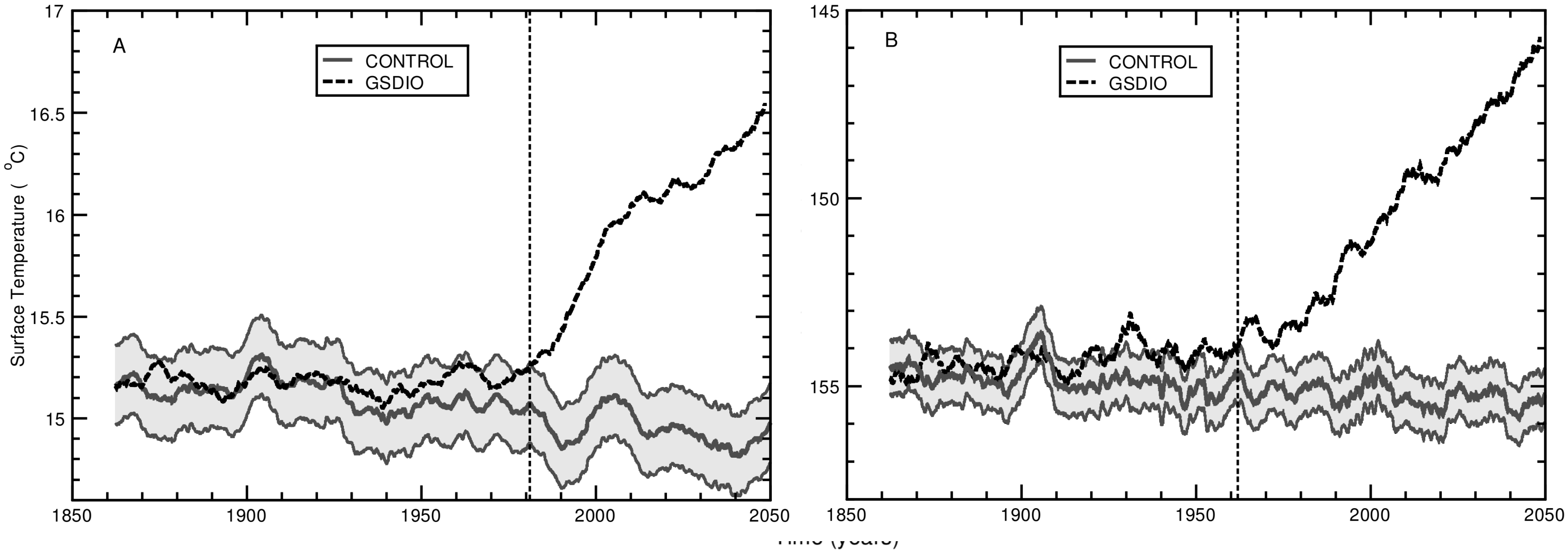

Figure3: Filtered global-mean monthly-mean near-surface temperature (panel A) and p_{LRT} (panel B) in the ECHAM GSDIO and control simulations. Data were smoothed with a 60-month moving average window; bold lines are the filtered values. The grey envelope denotes the $\pm 2\sigma$ 'noise envelope' in the control run data. Dashed vertical lines indicate the times at which the GSDIO surface temperature and p_{LRT} data separate from (and remain outside) the noise envelope. For display purposes, only the first 191 years of the 300-year control run are shown.

Sausen and Santer, 2003

Observed variations in regional temperatures since 1850

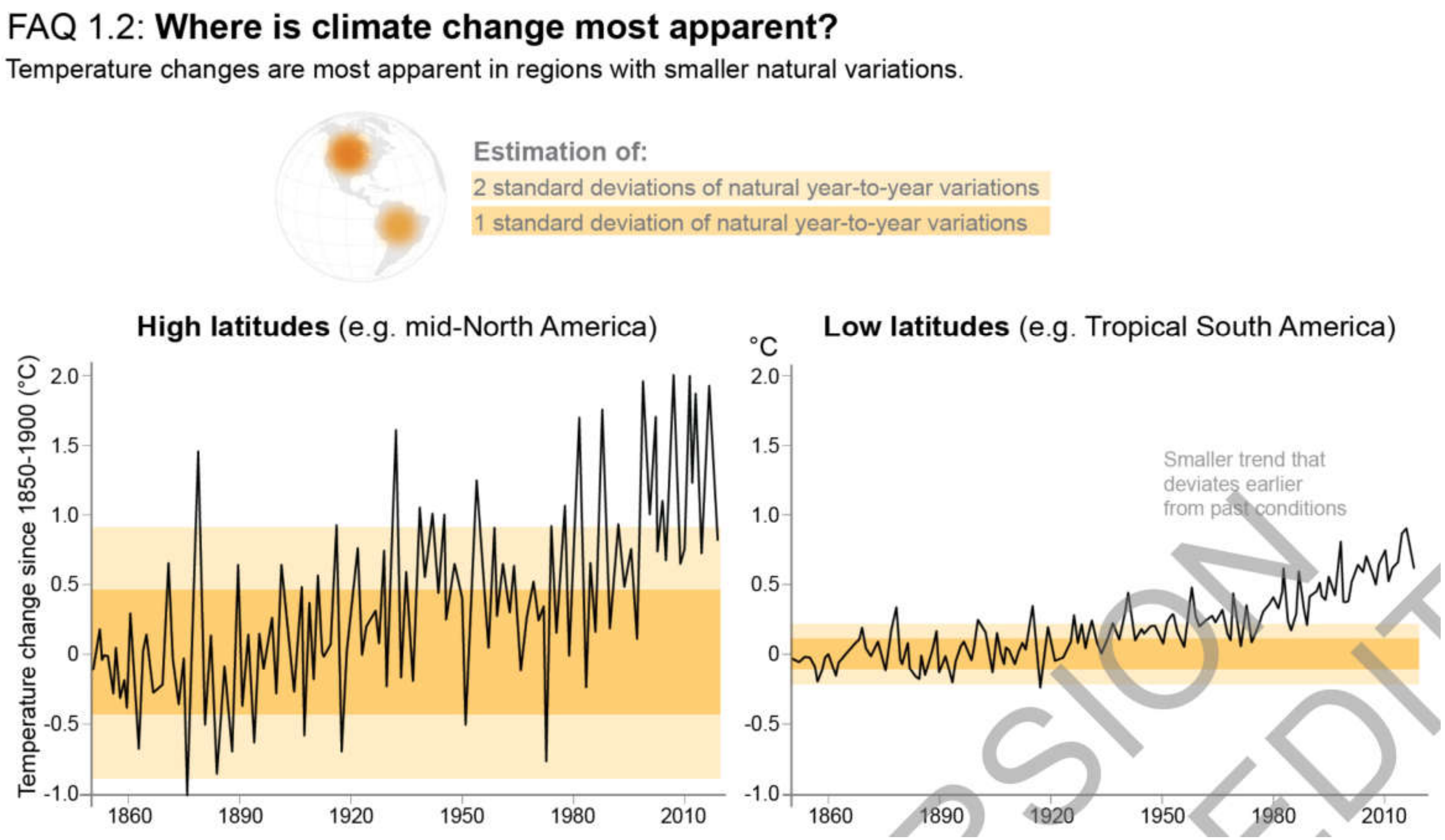

FAQ 1.2, Figure 1: Observed variations in regional temperatures since 1850 (data from Berkeley Earth). Regions in high latitudes, such as mid-North America (40°N–64°N, 140°W–60°W, left), have warmed by a larger amount than regions at lower latitudes, such as Tropical South America (10°S–10°N, 84°W–16°W, right), but the natural variations are also much larger at high latitudes (darker and lighter shading represents 1 and 2 standard deviations, respectively, of natural year-to-year variations). The signal of observed temperature change emerged earlier in Tropical South America than mid-North America even though the changes were of a smaller magnitude. (Note that those regions were chosen because of the longer length of their observational record, see Figure 1.14 for more regions).

IPCC 2021, Chap. 1

The observed emergence of changes in temperature.

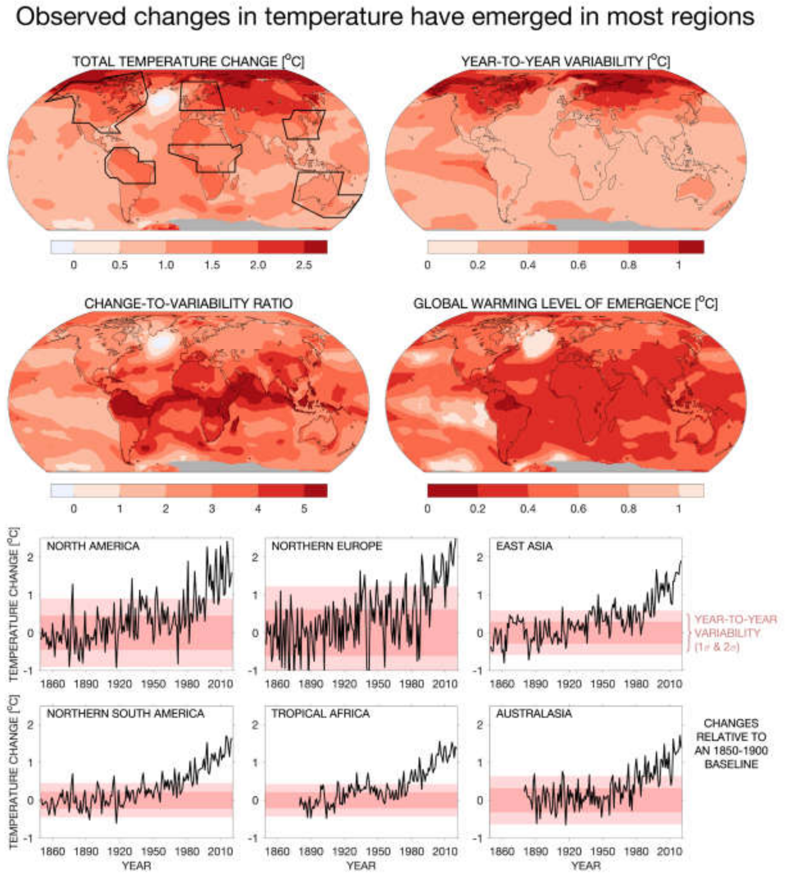

IPCC 2021, Chap. 1

Figure 1.14: The observed emergence of changes in temperature. Top left: the total change in temperature estimated for 2020 relative to 1850–1900 (following Hawkins et al. 2020), showing the largest warming in the Arctic. Top right: the amplitude of estimated year-to-year variations in temperature. Middle left: the ratio of the observed total change in temperature and the amplitude of temperature variability (the 'signal-to-noise (S/N) ratio'), showing that the warming is most apparent in the tropical regions (also see FAQ1.2). Middle right: the global warming level at which the change in local temperature becomes larger than the local year-to-year variability. The bottom panels show time series of observed annual mean surface air temperatures over land in various example regions, as indicated as boxes in the top left panel. The 1 and 2 standard deviations of estimated year-to-year variations for that region are shown by the pink shaded bands. Observed temperature data from Berkeley Earth (Rohde and Hausfather, 2020). Further details on data sources and processing are available in the chapter data table (Table 1.SM.1).

The observed emergence of changes in temperature.

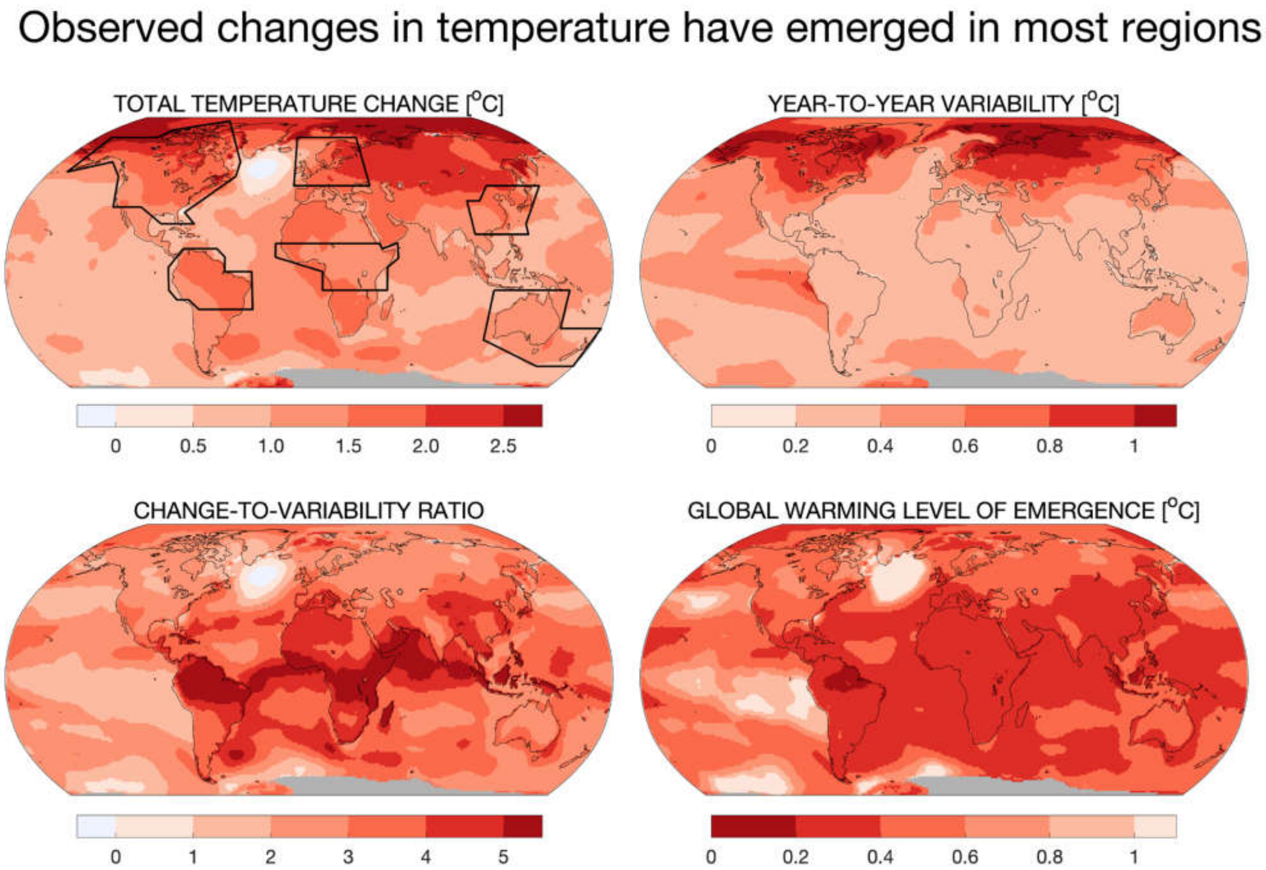

Figure 1.14: The observed emergence of changes in temperature. Top left: the total change in temperature estimated for 2020 relative to 1850–1900 (following Hawkins et al. 2020), showing the largest warming in the Arctic. Top right: the amplitude of estimated year-to-year variations in temperature. Middle left: the ratio of the observed total change in temperature and the amplitude of temperature variability (the 'signal-to-noise (S/N) ratio'), showing that the warming is most apparent in the tropical regions (also see FAQ1.2). Middle right: the global warming level at which the change in local temperature becomes larger than the local year-to-year variability. The bottom panels show time series of observed annual mean surface air temperatures over land in various example regions, as indicated as boxes in the top left panel. The 1 and 2 standard deviations of estimated year-to-year variations for that region are shown by the pink shaded bands. Observed temperature data from Berkeley Earth (Rohde and Hausfather, 2020). Further details on data sources and processing are available in the chapter data table (Table 1.SM.1).

IPCC 2021, Chap. 1

The observed emergence of changes in temperature.

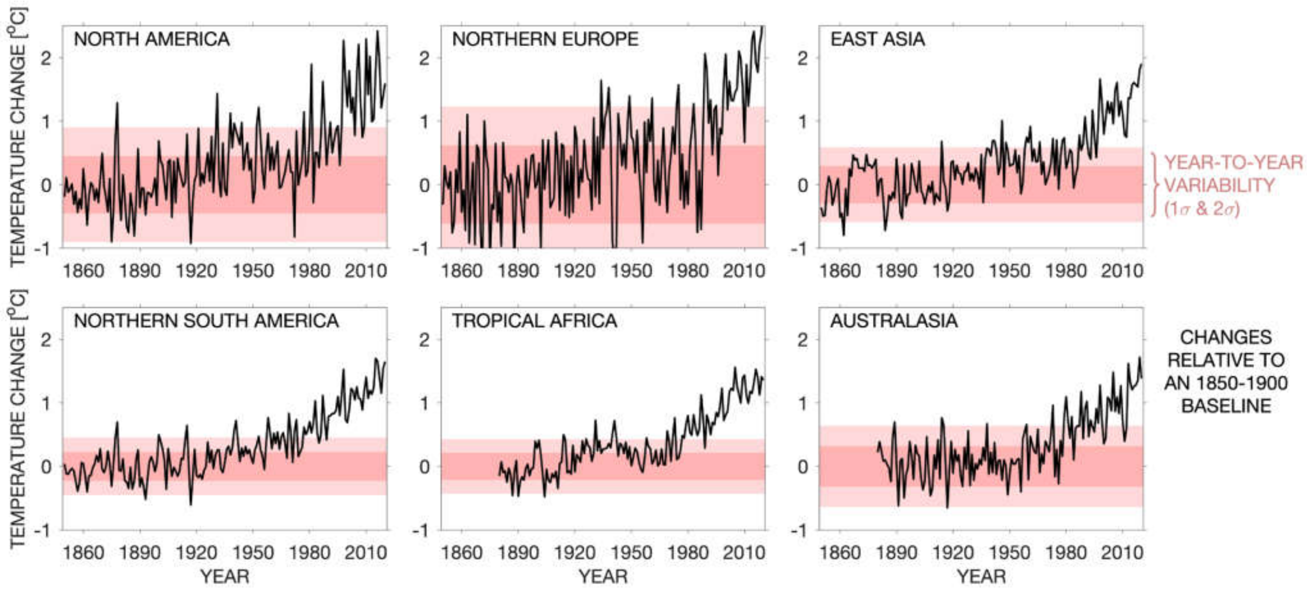

Figure 1.14: The observed emergence of changes in temperature. Top left: the total change in temperature estimated for 2020 relative to 1850–1900 (following Hawkins et al. 2020), showing the largest warming in the Arctic. Top right: the amplitude of estimated year-to-year variations in temperature. Middle left: the ratio of the observed total change in temperature and the amplitude of temperature variability (the 'signal-to-noise (S/N) ratio'), showing that the warming is most apparent in the tropical regions (also see FAQ1.2). Middle right: the global warming level at which the change in local temperature becomes larger than the local year-to-year variability. The bottom panels show time series of observed annual mean surface air temperatures over land in various example regions, as indicated as boxes in the top left panel. The 1 and 2 standard deviations of estimated year-to-year variations for that region are shown by the pink shaded bands. Observed temperature data from Berkeley Earth (Rohde and Hausfather, 2020). Further details on data sources and processing are available in the chapter data table (Table 1.SM.1).

IPCC 2021, Chap. 1

The ‘cascade of uncertainties’ in CMIP6 projections

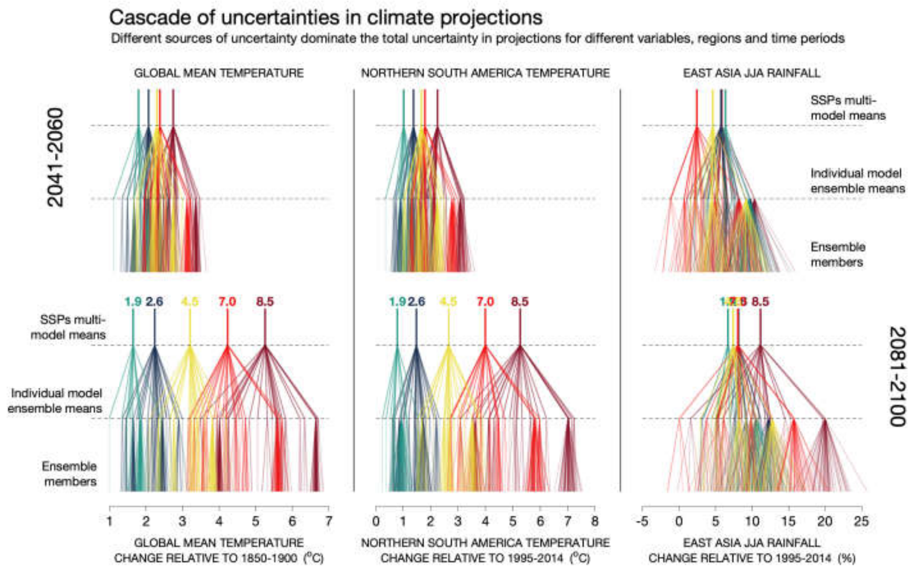

Figure 1.15: The ‘cascade of uncertainties’ in CMIP6 projections. Changes in GSAT (left), northern South America (region NSA) temperature change (middle), and East Asia (region EAS) summer (JJA) precipitation change (right) are shown for two time periods (2041–2060, top, and 2081–2100, bottom). The SSP-radiative forcing combination is indicated at the top of each cascade at the value of the multi-model mean for each scenario. This branches downwards to show the ensemble mean for each model, and further branches into the individual ensemble members, although often only a single member is available. These diagrams highlight the relative importance of different sources of uncertainty in climate projections, which varies for different time periods, regions and climate variables. See Section 1.4.5 for the definition of the regions used. Further details on data sources and processing are available in the chapter data table (Table 1.SM.1).

IPCC 2021, Chap. 1

Cascade of uncertainties in climate projections

Different sources of uncertainty dominate the total uncertainty in projections for different variables, regions and time periods

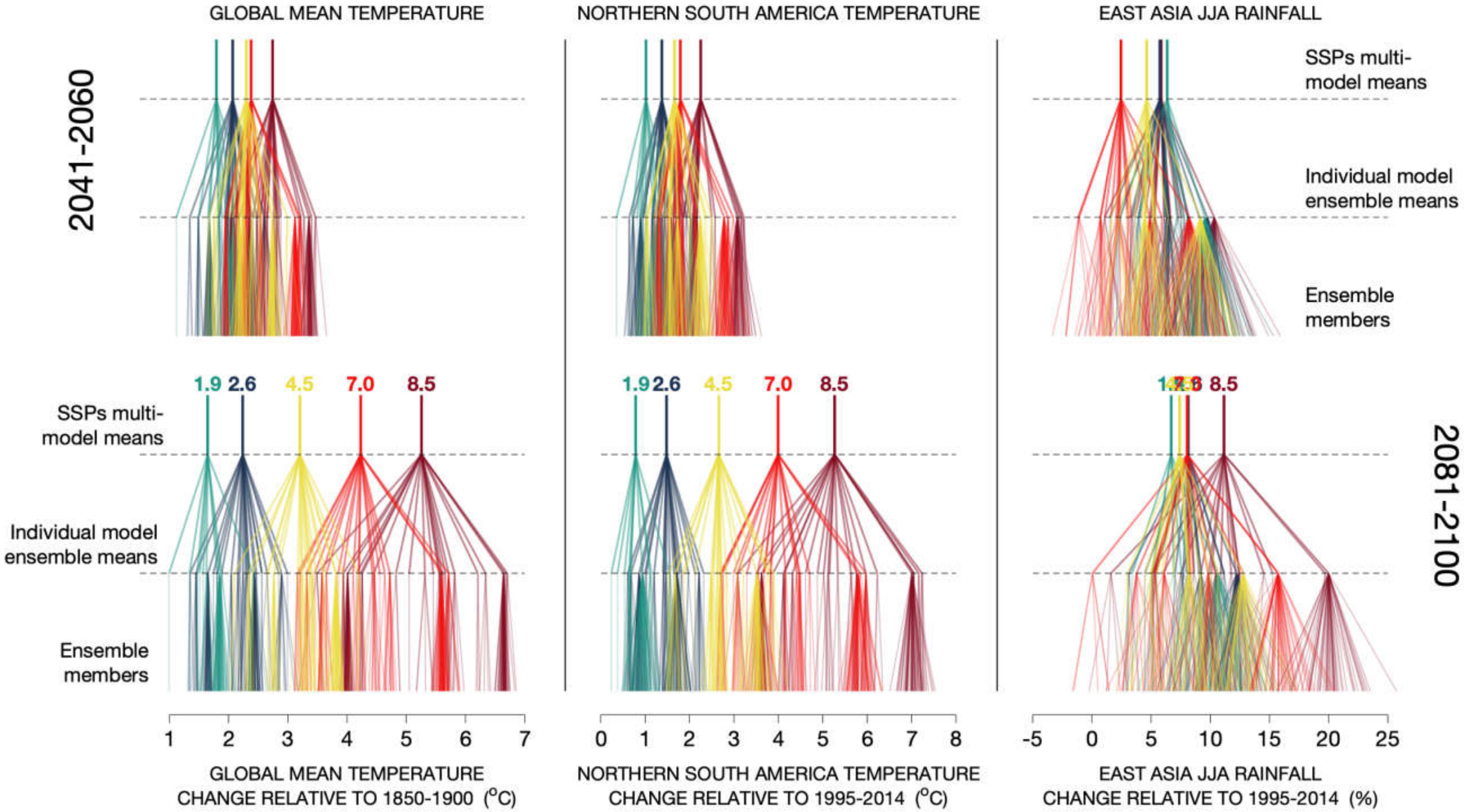

Statements in the Executive Summary

Framing and Context of the WGI Report (7)

The AR6 has adopted a unified framework of climate risk, supported by an increased focus in WGI on low-likelihood, high-impact events. Systematic risk framing is intended to aid the formulation of effective responses to the challenges posed by current and future climatic changes and to better inform risk assessment and decision-making. AR6 also makes use of the ‘storylines’ approach, which contributes to building a robust and comprehensive picture of climate information, allows a more flexible consideration and communication of risk, and can explicitly address low-likelihood, high-impact events. {1.1.2, 1.4.4, Cross-Chapter Box 1.3}

IPCC 2021, Chap. 1

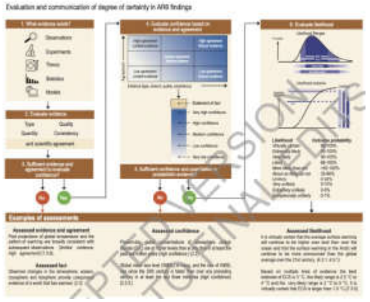

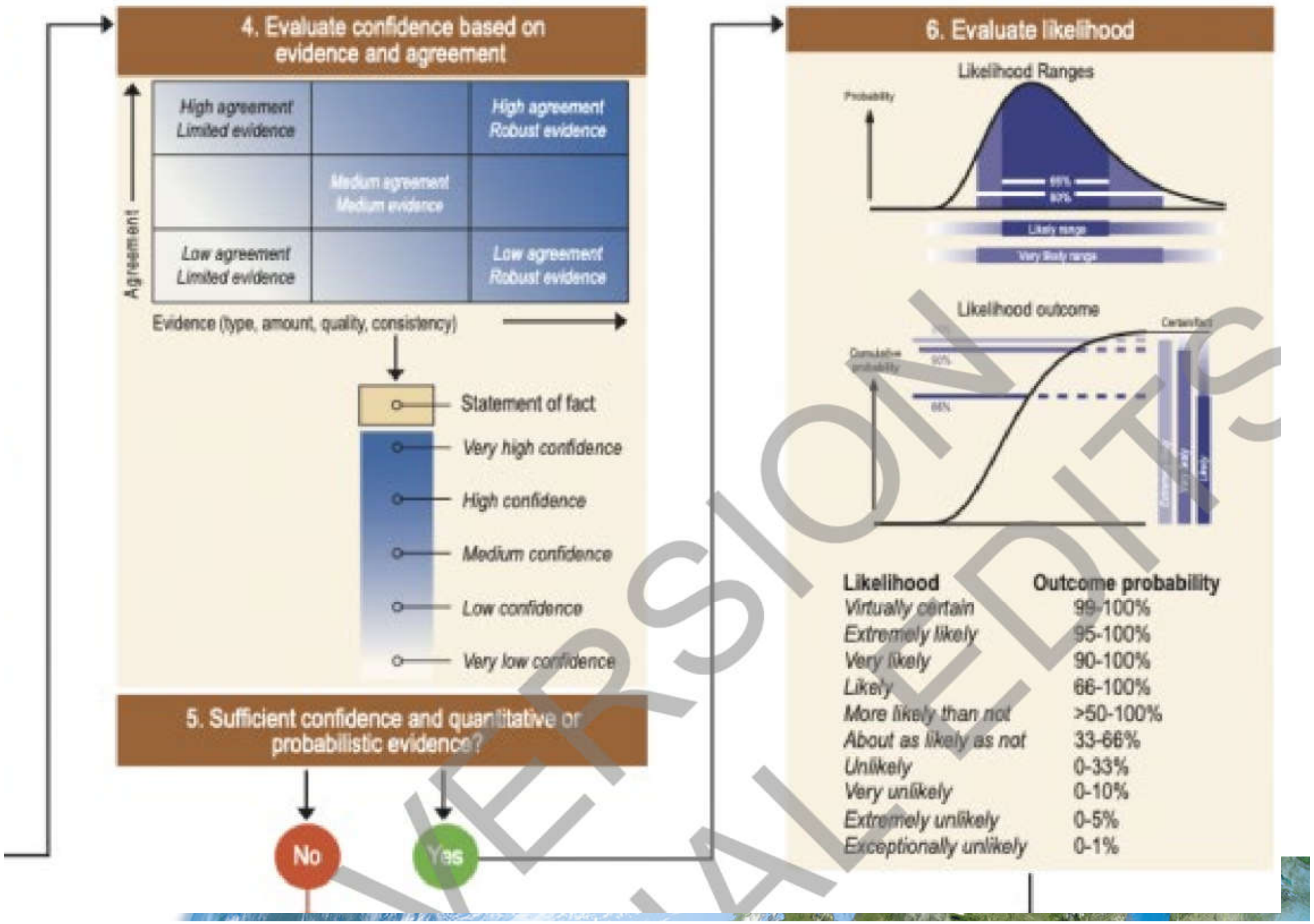

4. Evaluate confidence based on evidence and agreement
High agreement Limited evidence
High agreement Robust evidence
Medium agreement Medium evidence
Low agreement Limited evidence
Low agreement Robust evidence
Agreement
Evidence (type, amount, quality, consistency)
Statement of fact
Very high confidence
High confidence
Medium confidence
Low confidence
Very low confidence
5. Sufficient confidence and quantitative or probabilistic evidence?
No
Yes
6. Evaluate likelihood
Likelihood Ranges
Probability
66%
90%
Likely range
Very likely range
Likelihood outcome
Certain fact
Cumulative probability
90%
66%
Likelihood
Outcome probability
Virtually certain
99-100%
Extremely likely
95-100%
Very likely
90-100%
Likely
66-100%
More likely than not
>50-100%
About as likely as not
33-66%
Unlikely
0-33%
Very unlikely
0-10%
Extremely unlikely
0-5%
Exceptionally unlikely
0-1%

Illustrating concepts of low-likelihood scenarios

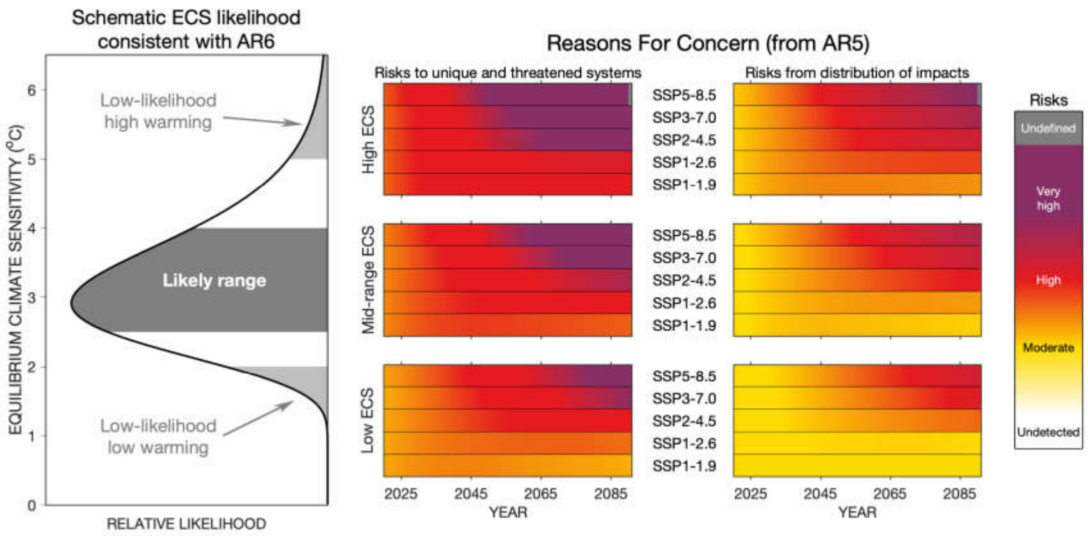

IPCC 2021, Chap. 1

Figure 1.16: Illustrating concepts of low-likelihood scenarios. Left: schematic likelihood distribution consistent with the IPCC AR6 assessments that equilibrium climate sensitivity (ECS) is *likely* in the range 2.5 to 4.0°C, and *very likely* between 2.0 and 5.0°C (Chapter 7). ECS values outside the assessed *very likely* range are designated low-likelihood scenarios in this example (light grey). Middle and right columns: additional risks due to climate change for 2020–2090 using the Reasons For Concern (RFCs, see IPCC, 2014), specifically RFC1 describing the risks to unique and threatened systems and RFC3 describing risks from the distribution of impacts (O'Neill et al., 2017; Zommers et al., 2020). The projected changes of GSAT used are the 95%, median and 5% assessed ranges from Chapter 4 for each SSP (top, middle and bottom); these are designated High ECS, Mid-range ECS and Low ECS respectively. The burning-ember risk spectrum is usually associated with levels of committed GSAT change; instead, this illustration associates the risk spectrum with the GSAT temperature reached in each year from 2020 to 2090. Note that this illustration does not include the vulnerability aspect of each SSP scenario. Further details on data sources and processing are available in the chapter data table (Table 1.SM.1).

Illustrating concepts of low-likelihood scenarios

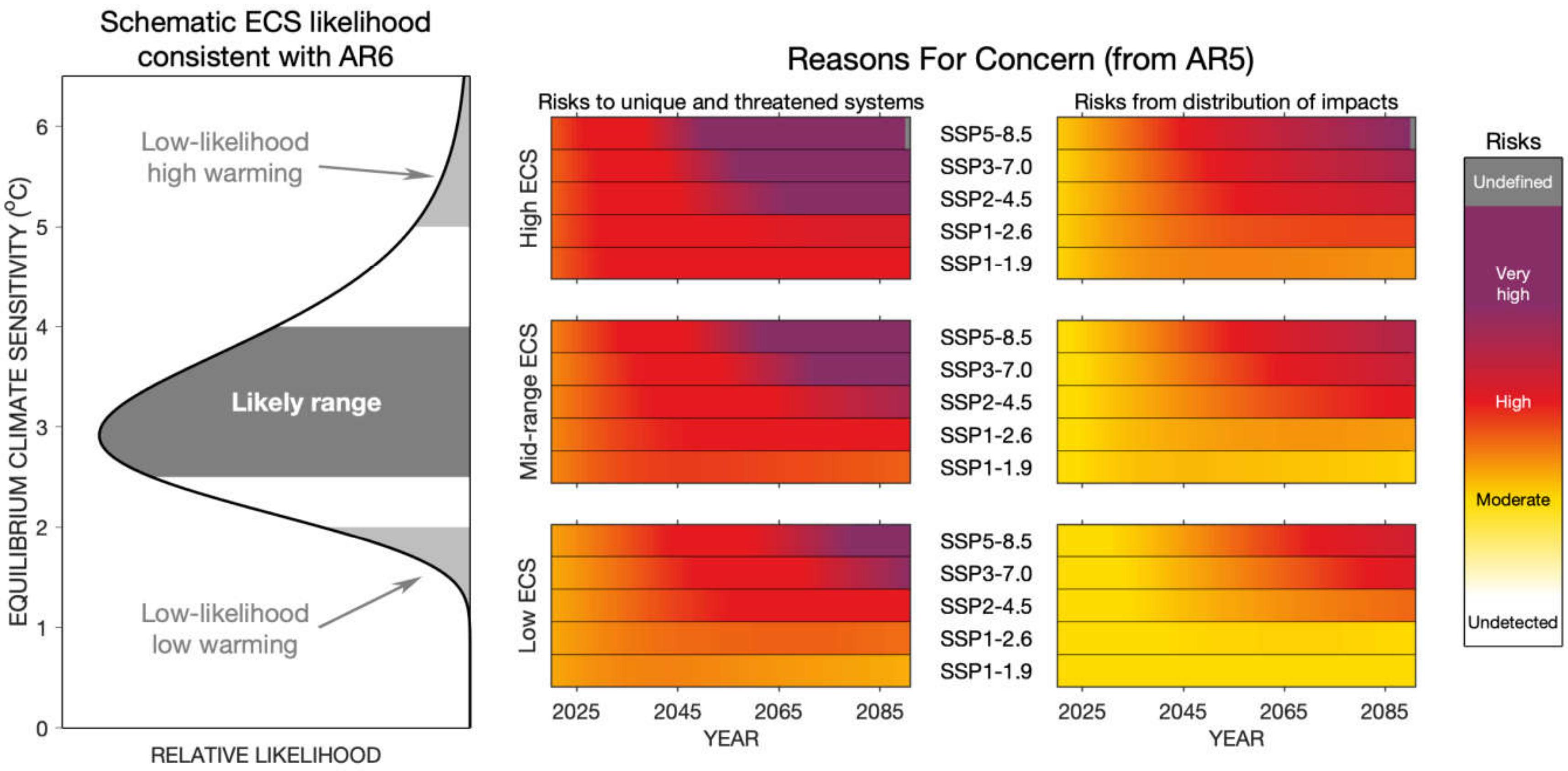

Illustration of two types of tipping points: noise-induced and bifurcation

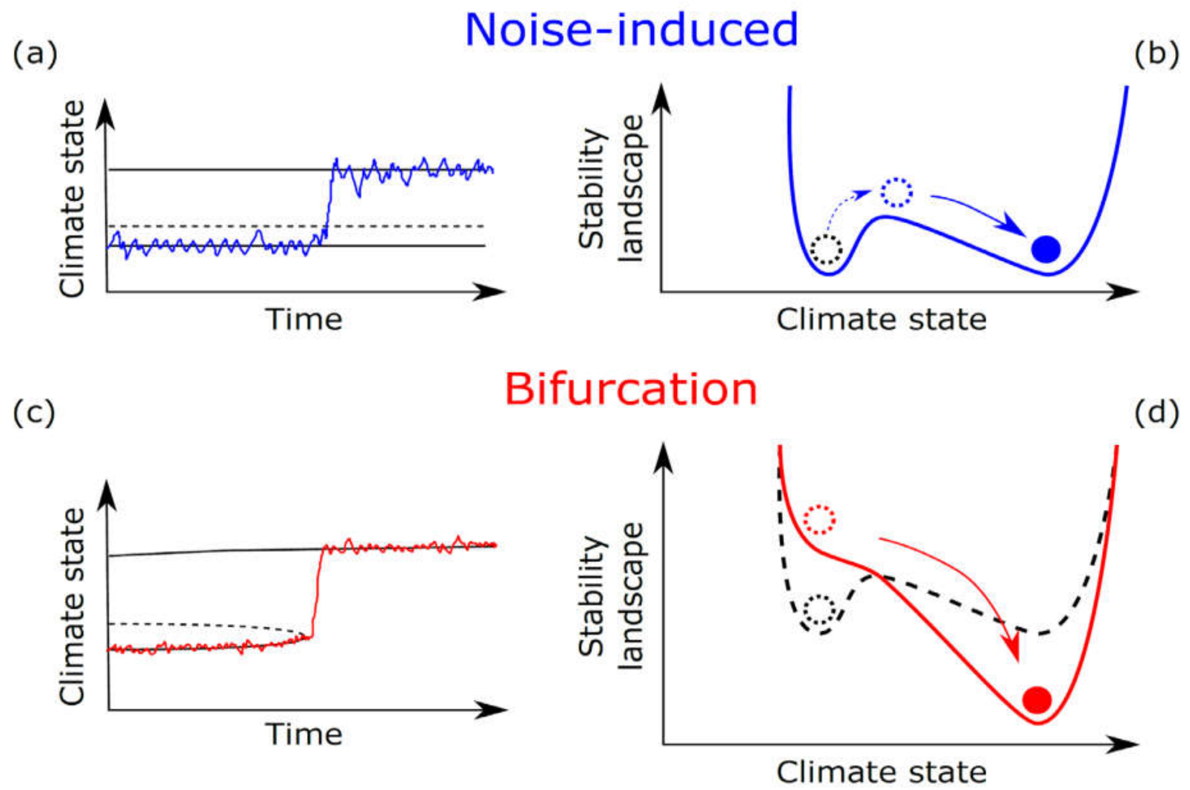

IPCC 2021, Chap. 1


Figure 1.17: Illustration of two types of tipping points: noise-induced (panels a, b) and bifurcation (panels c, d). (a), (c) example time-series (coloured lines) through the tipping point with black solid lines indicating stable climate states (e.g., low or high rainfall) and dashed lines represent the boundary between stable states. (b), (d) stability landscapes provide an intuitive understanding for the different types of tipping point. The valleys represent different climate states the system can occupy, with hill tops separating the stable states. The resilience of a climate state is implied by the depth of the valley. The current state of the system is represented by a ball. Both scenarios assume that the ball starts in the left-hand valley (black dashed lines) and then through different mechanisms dependent on the type of tipping transitions to the right valley (coloured lines). Noise-induced tipping events, for instance drought events causing sudden dieback of the Amazonian rainforest, develop from fluctuations within the system. The stability landscape in this scenario remains fixed and stationary. A series of perturbations in the same direction or one large perturbation are required to force the system over the hill top and into the alternative stable state. Bifurcation tipping events, such as a collapse of the thermohaline circulation in the Atlantic Ocean under climate change, occur when a critical level in the forcing is reached. Here the stability landscape is subjected to a change in shape. Under gradual anthropogenic forcing the left valley begins to shallow and eventually vanishes at the tipping point, forcing the system to transition to the right-hand valley.

Statements in the Executive Summary

Framing and Context of the WGI Report (8)

The construction of climate change information and communication of scientific understanding are influenced by the values of the producers, the users and their broader audiences. Scientific knowledge interacts with pre-existing conceptions of weather and climate, including values and beliefs stemming from ethnic or national identity, traditions, religion or lived relationships to land and sea (*high confidence*). Science has values of its own, including objectivity, openness and evidence-based thinking. Social values may guide certain choices made during the construction, assessment and communication of information (*high confidence*). {1.2.3, Box 1.1}

IPCC 2021, Chap. 1

Choice of baseline matters
when comparing observations and model simulations

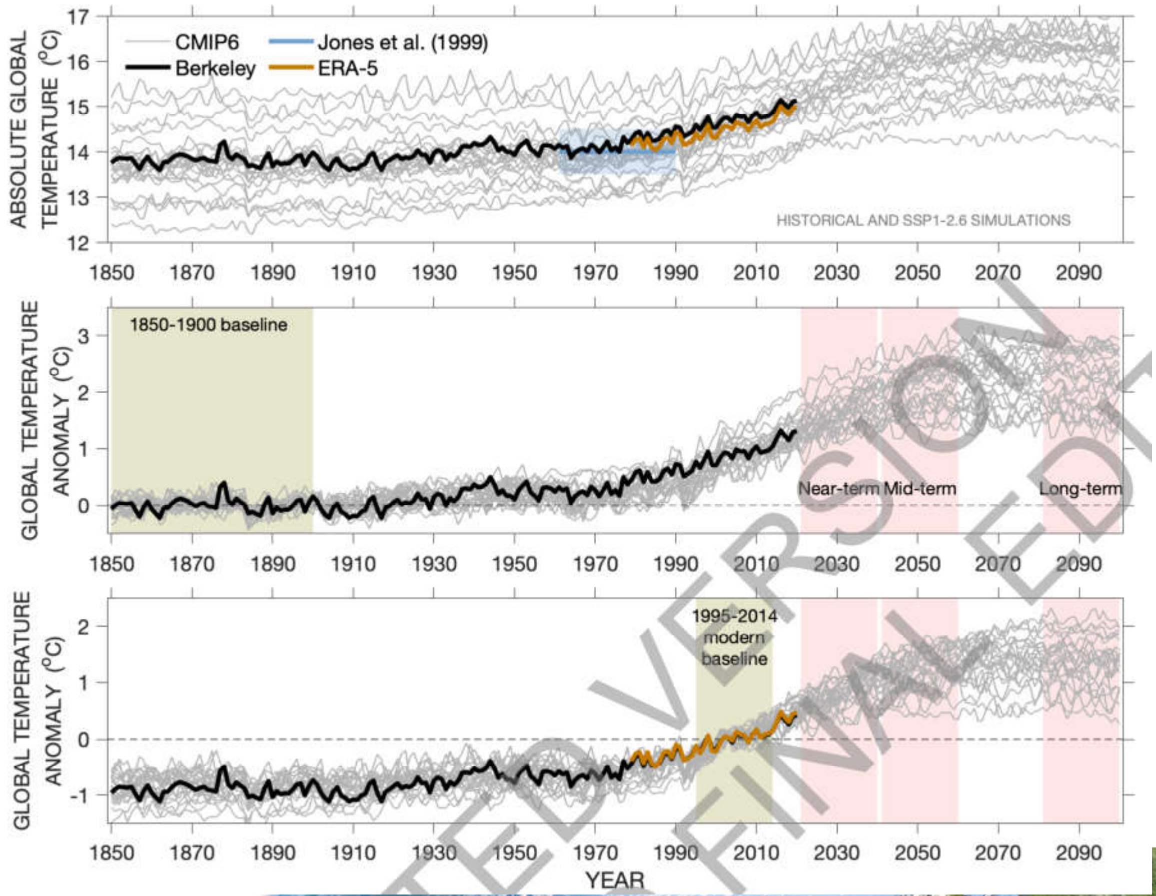

Figure 1.11: Choice of baseline matters when comparing observations and model simulations. Global mean surface air temperature (GSAT, grey) from a range of CMIP6 historical simulations (1850–2014, 25 models) and SSP1-2.6 (2015–2100) using absolute values (top) and anomalies relative to two different baselines: 1850–1900 (middle) and 1995–2014 (bottom). An estimate of GSAT from a reanalysis (ERA-5, orange, 1979–2020) and an observation-based estimate of global mean surface air temperature (GMST) (Berkeley Earth, black, 1850–2020) are shown, along with the mean GSAT for 1961–1990 estimated by Jones et al. (1999), light blue shading, 14.0±0.5°C). Using the more recent baseline (bottom) allows the inclusion of datasets which do not include the periods of older baselines. The middle and bottom panels have scales which are the same size but offset. Further details on data sources and processing are available in the chapter data table (Table 1.SM.1).

IPCC 2021, Chap. 1

Statements in the Executive Summary

Data, Tools and Methods Used across the WGI Report (1)

Capabilities for observing the physical climate system have continued to improve and expand overall, but some reductions in observational capacity are also evident (*high confidence*). Improvements are particularly evident in ocean observing networks and remote-sensing systems, and in paleoclimate reconstructions from proxy archives. However, some climate-relevant observations have been interrupted by the discontinuation of surface stations and radiosonde launches, and delays in the digitisation of records. Further reductions are expected to result from the COVID-19 pandemic. In addition, paleoclimate archives such as mid-latitude and tropical glaciers as well as modern natural archives used for calibration (e.g., corals and trees) are rapidly disappearing owing to a host of pressures, including increasing temperatures (*high confidence*). {1.5.1}

IPCC 2021, Chap. 1

Temporal coverage of selected instrumental climate observations (top) and selected paleoclimate archives (bottom)

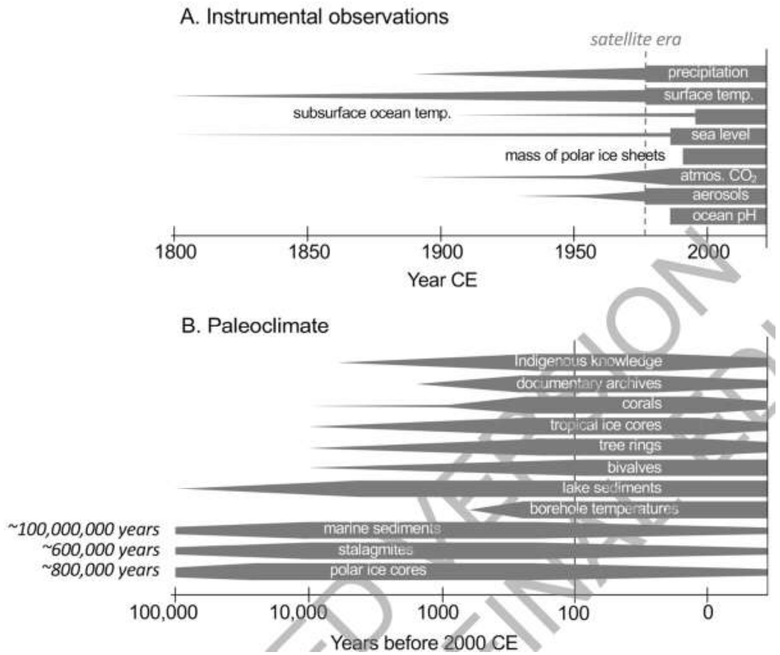

Figure 1.7: Schematic of temporal coverage of selected instrumental climate observations (top) and selected paleoclimate archives (bottom). The satellite era began in 1979 CE (Common Era). The width of the taper gives an indication of the amount of available records.

IPCC 2021, Chap. 1

Temporal coverage of selected instrumental climate observations (top) and selected paleoclimate archives (bottom)

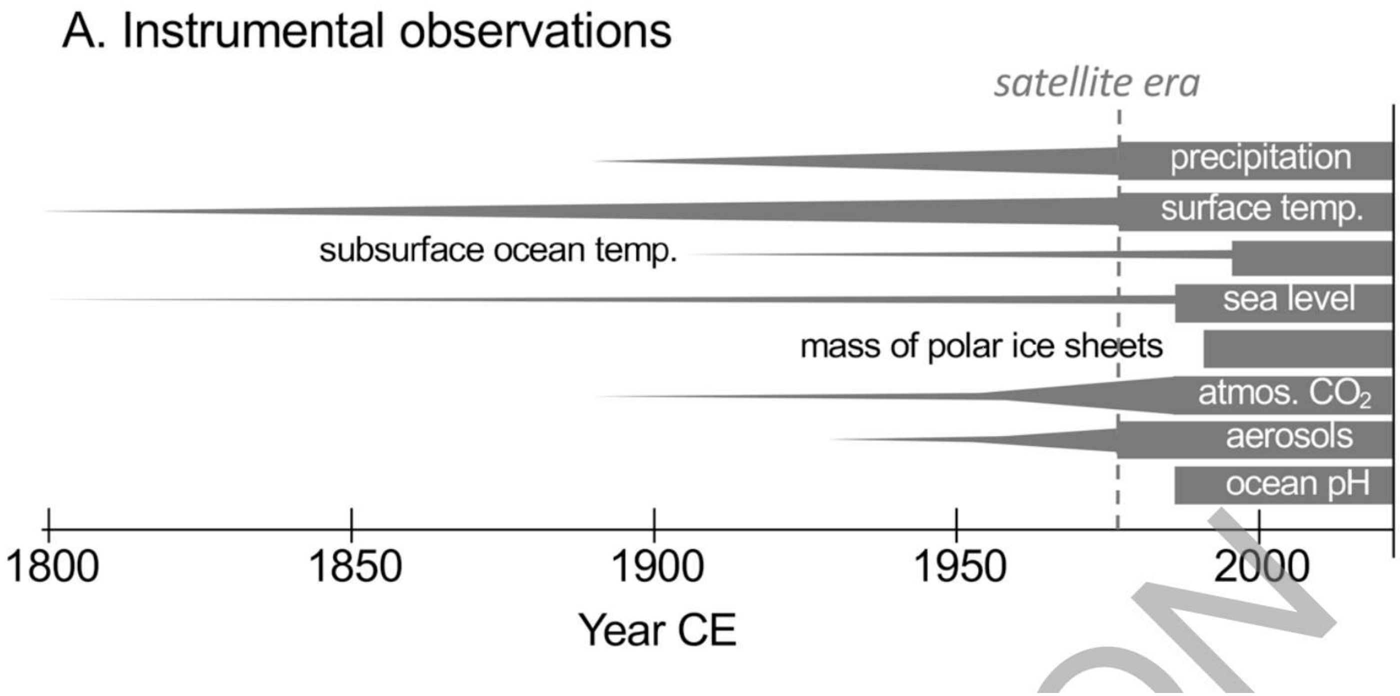

CE = Common Era

IPCC 2021, Chap. 1

Temporal coverage of selected instrumental climate observations (top) and selected paleoclimate archives (bottom)

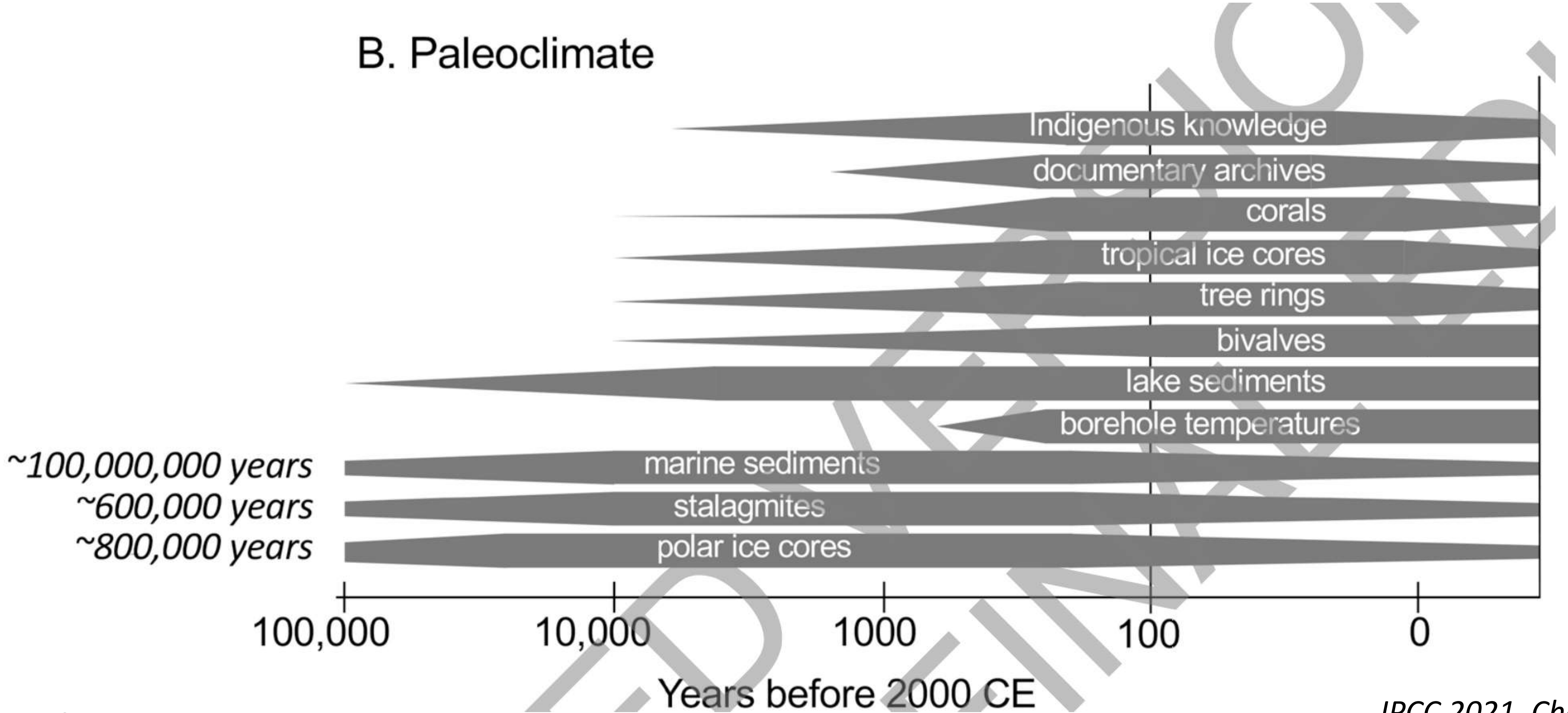

IPCC 2021, Chap. 1

Statements in the Executive Summary

Data, Tools and Methods Used across the WGI Report (2)

Reanalyses have improved since AR5 and are increasingly used as a line of evidence in assessments of the state and evolution of the climate system (*high confidence*). Reanalyses, where atmosphere or ocean forecast models are constrained by historical observational data to create a climate record of the past, provide consistency across multiple physical quantities and information about variables and locations that are not directly observed. Since AR5, new reanalyses have been developed with various combinations of increased resolution, extended records, more consistent data assimilation, estimation of uncertainty arising from the range of initial conditions, and an improved representation of the ocean. While noting their remaining limitations, the WGI report uses the most recent generation of reanalysis products alongside more standard observation-based datasets. {1.5.2, Annex 1}

IPCC 2021, Chap. 1

Statements in the Executive Summary

Data, Tools and Methods Used across the WGI Report (3)

Since AR5, new techniques have provided greater confidence in attributing changes in climate extremes to climate change. Attribution is the process of evaluating the relative contributions of multiple causal factors to an observed change or event. This includes the attribution of the causal factors of changes in physical or biogeochemical weather or climate variables (e.g., temperature or atmospheric CO_2) as done in, or of the impacts of these changes on natural and human systems (e.g., infrastructure damage or agricultural productivity), as done in WGII. Attributed causes include human activities (such as emissions of greenhouse gases and aerosols, or land-use change), and changes in other aspects of the climate, or natural or human systems. {Cross-WG Box 1.1}

IPCC 2021, Chap. 1

Statements in the Executive Summary

Data, Tools and Methods Used across the WGI Report (4)

The latest generation of complex climate models has an improved representation of physical processes, and a wider range of Earth system models now represent biogeochemical cycles. Since the AR5, higher-resolution models that better capture smaller-scale processes and extreme events have become available. Key model intercomparisons supporting this assessment include the Coupled Model Intercomparison Project Phase 6 (CMIP6) and the Coordinated Regional Climate Downscaling Experiment (CORDEX), for global and regional models respectively. Results using CMIP Phase 5 (CMIP5) simulations are also assessed. Since the AR5, large ensemble simulations, where individual models perform multiple simulations with the same climate forcings, are increasingly used to inform understanding of the relative roles of internal variability and forced change in the climate system, especially on regional scales. The broader availability of ensemble model simulations has contributed to better estimations of uncertainty in projections of future change (*high confidence*). A broad set of simplified climate models is assessed and used as emulators to transfer climate information across research communities, such as for evaluating impacts or mitigation pathways consistent with certain levels of future warming. {1.4.2, 1.5.3, 1.5.4, Cross-chapter Box 30 7.1}

IPCC 2021, Chap. 1

A world map showing the increased diversity of modelling centres contributing to CMIP and CORDEX

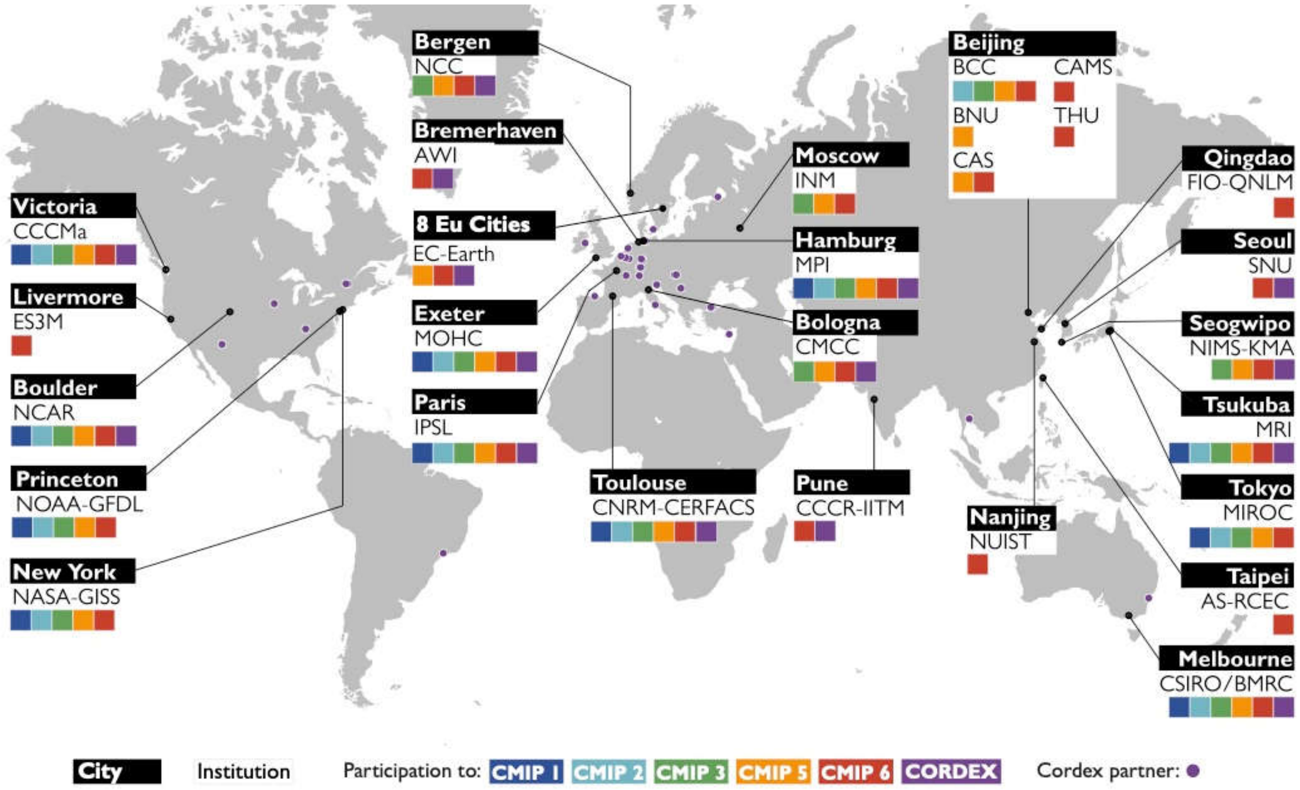

Figure 1.20: A world map showing the increased diversity of modelling centres contributing to CMIP and CORDEX. Climate models are often developed by international consortia. EC-Earth is shown as an example (involving SMHI, Sweden; KNMI, The Netherlands; DMI, Denmark; AEMET, Spain; Met Éireann, Ireland; CNR-ISAC, Italy; Instituto de Meteorologia, Portugal; FMI, Finland), but there are too many such collaborations to display all of them on this map. More complete information about institutions contributing to CORDEX and CMIP6 is found in Annex II.

IPCC 2021, Chap. 1

Structure of CMIP6, the 6th phase of the Coupled Model Intercomparison Project

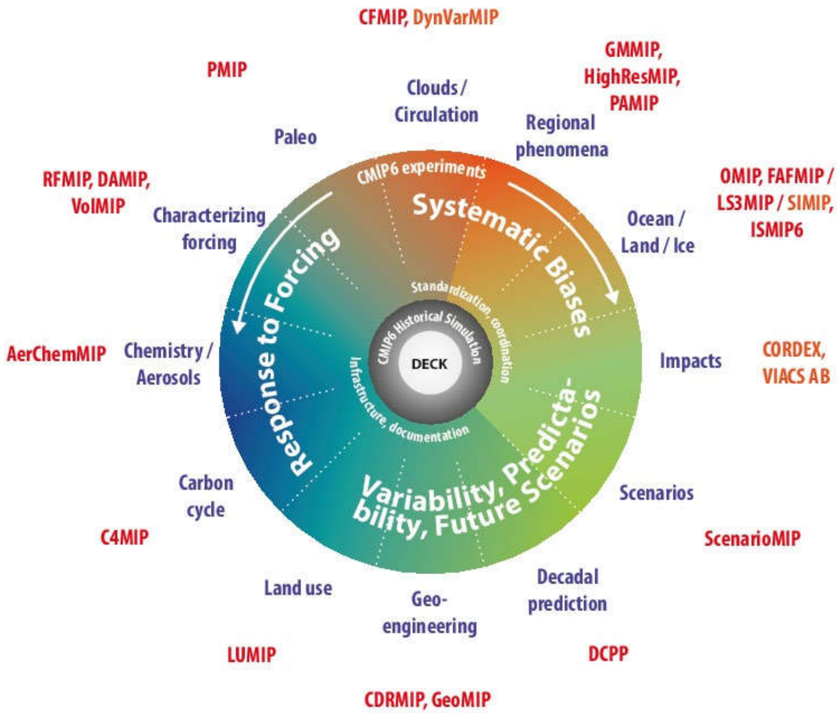

IPCC 2021, Chap. 1

Figure 1.22: Structure of CMIP6, the 6th phase of the Coupled Model Intercomparison Project. The centre shows the common DECK (Diagnostic, Evaluation and Characterization of Klima) and historical experiments that all participating models must perform. The outer circles show the topics covered by the endorsed (blue) and other MIPs (red). See Table 1.3 for explanation of the MIP acronyms. (expanded from Eyring et al., 2016).

Resolution of the atmospheric and oceanic components of global climate models participating in CMIP5, CMIP6, and HighResMIP

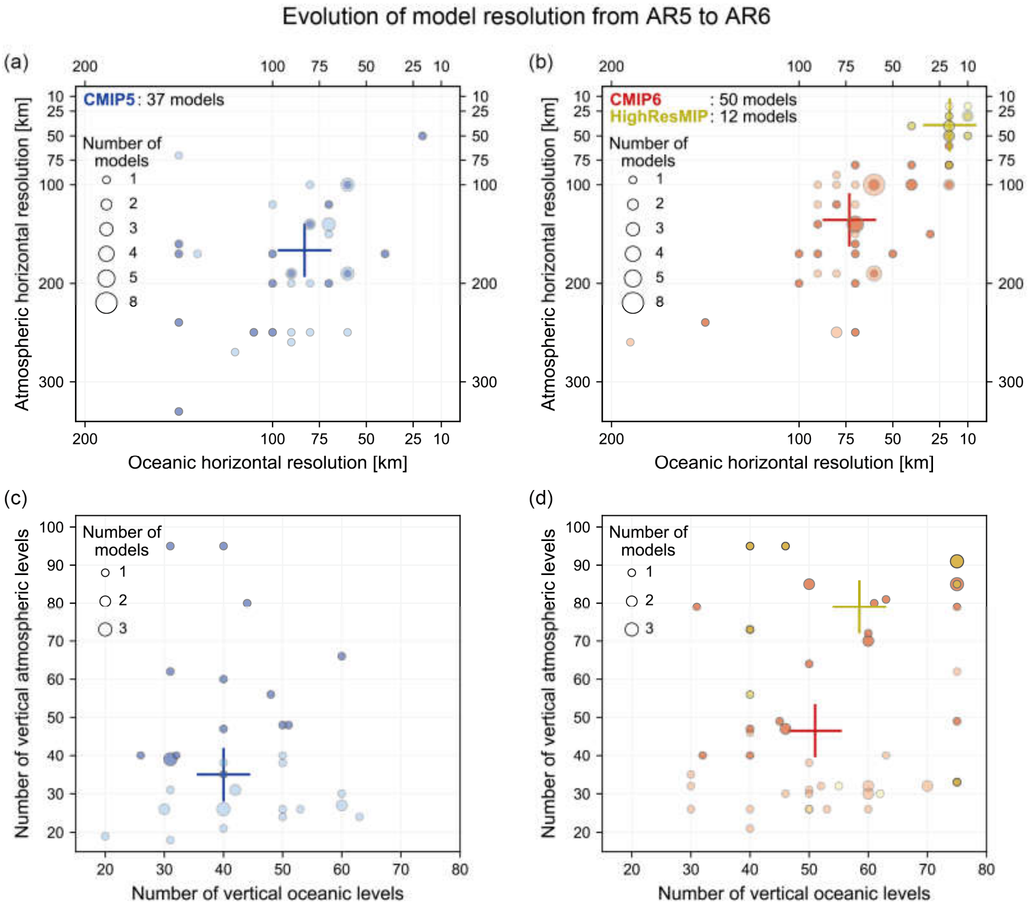

Figure 1.19: Resolution of the atmospheric and oceanic components of global climate models participating in CMIP5, CMIP6, and HighResMIP: (a) (b) horizontal resolution (km), and (c) (d) number of vertical levels. Darker colour circles indicate high-top models (whose top of the atmosphere is above 50 km). The crosses are the median values. These models are documented in Annex II. Note that duplicated models in a modelling group are counted as one entry when their horizontal and vertical resolutions are same. For HighResMIP, one atmosphere-ocean coupled model with the highest resolution from each modelling group is used. The horizontal resolution (rounded to 10km) is the square root of the number of grid points divided by the surface area of the Earth, or the number of surface ocean grid points divided by the area of the ocean surface, for the atmosphere and ocean respectively.

IPCC 2021, Chap. 1

Illustration of common types of model ensemble, simulating the time evolution of a quantity Q

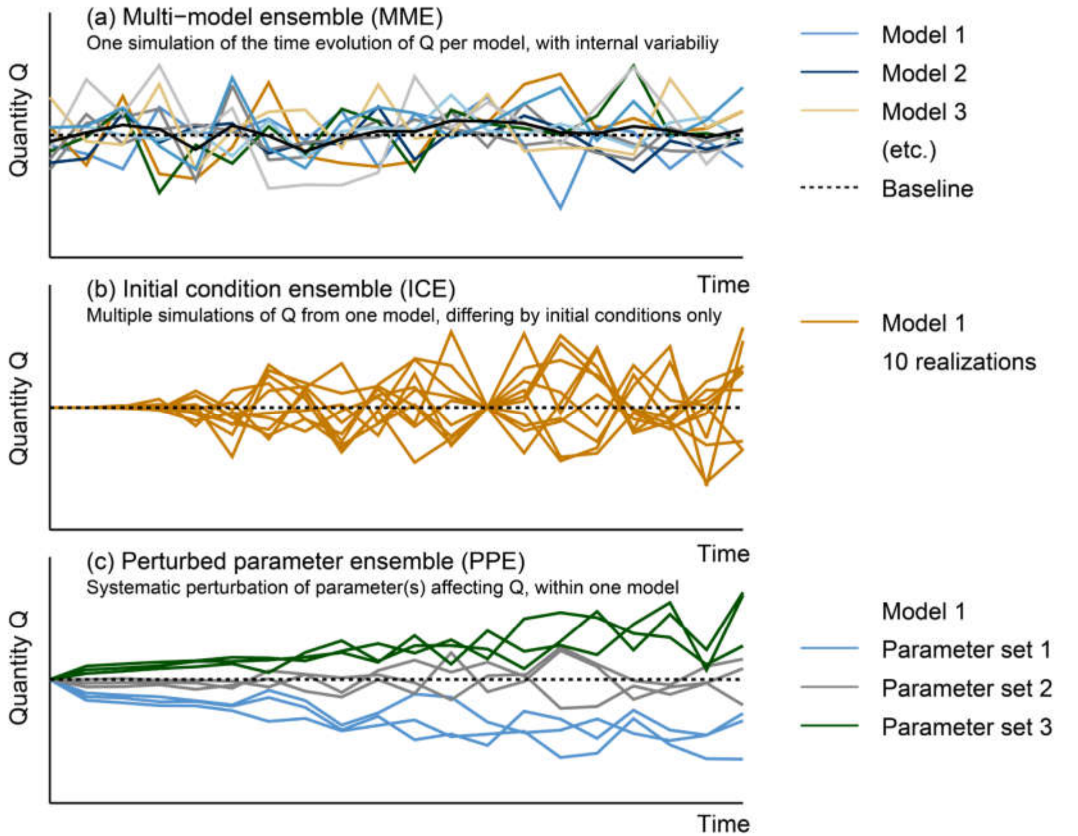

Figure 1.21: Illustration of common types of model ensemble simulating the time evolution of a quantity Q (such as global mean surface temperature). (a) Multi-model ensemble, where each model has its own realization of the processes affecting Q, and its own internal variability around the baseline value (dashed line). The multi-model mean (black) is commonly taken as the ensemble average. (b) Initial condition ensemble, where several realizations from a single model are compared. These differ only by minute ('micro') perturbations to the initial conditions of the simulation, such that over time, internal variability will progress differently in each ensemble member. (c) Perturbed physics ensemble, which also compares realizations from a single model, but where one or more internal parameters that may affect the simulations of Q are systematically changed to allow for a quantification of the impact of those quantities on the model results. Additionally, each parameter set may be taken as the starting point for an initial condition ensemble. In this figure, each set has three ensemble members.

IPCC 2021, Chap. 1

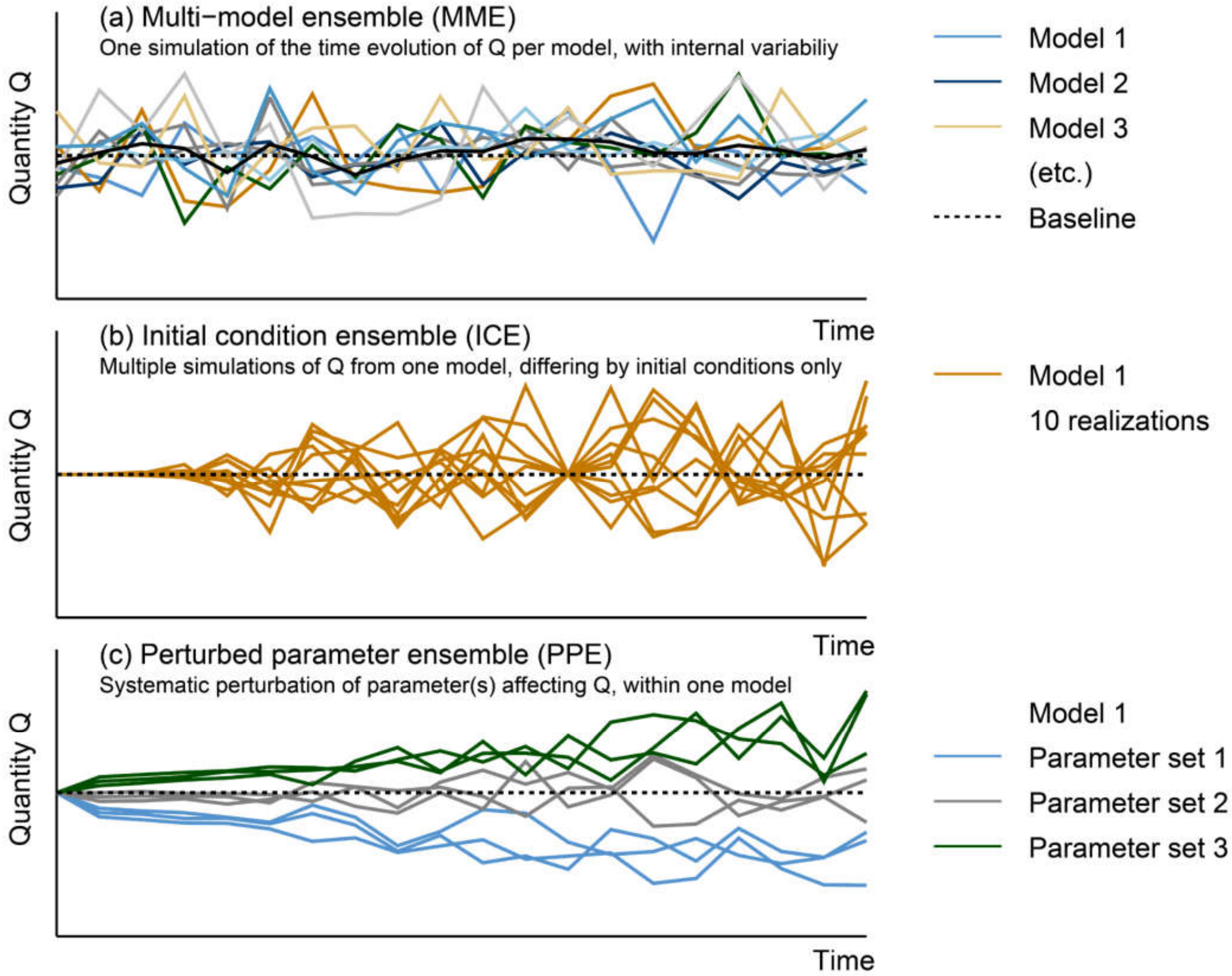

IPCC 2021, Chap. 1

Statements in the Executive Summary

Data, Tools and Methods Used across the WGI Report (5)

Assessments of future climate change are integrated within and across the three IPCC Working Groups through the use of three core components: scenarios, global warming levels, and the relationship between cumulative carbon emissions and global warming. Scenarios have a long history in the IPCC as a method for systematically examining possible futures. A new set of scenarios, derived from the Shared Socio-economic Pathways (SSPs), is used to synthesize knowledge across the physical sciences, impact, and adaptation and mitigation research. The core set of SSP scenarios used in the WGI report, SSP1-1.9, SSP1-2.6, SSP2-4.5, SSP3-7.0 and SSP5-8.5, cover a broad range of emission pathways, including new low-emissions pathways. The feasibility or likelihood of individual scenarios is not part of this assessment, which focuses on the climate response to possible, prescribed emission futures. Levels of global surface temperature change (global warming levels), which are closely related to a range of hazards and regional climate impacts, also serve as reference points within and across IPCC Working Groups. Cumulative carbon emissions, which have a nearly linear relationship to increases in global surface temperature, are also used. {1.6.1-1.6.4, Cross-Chapter Box 1.5, Cross-Chapter Box 11.1}

IPCC 2021, Chap. 1

A simplified illustration of the scenario generation

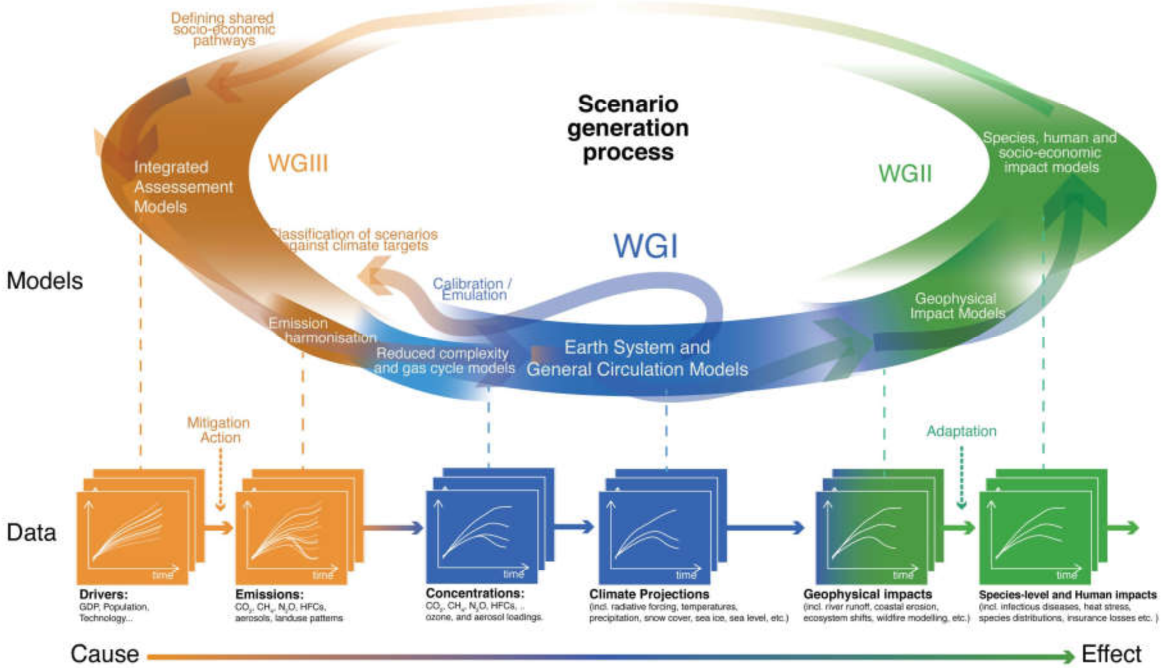

Figure 1.27: A simplified illustration of the scenario generation process that involves the scientific communities represented in the three IPCC Working Groups. The circular set of arrows at the top indicate the main set of models and workflows used in that scenario generation process, with the lower level indicating the datasets.

IPCC 2021, Chap. 1

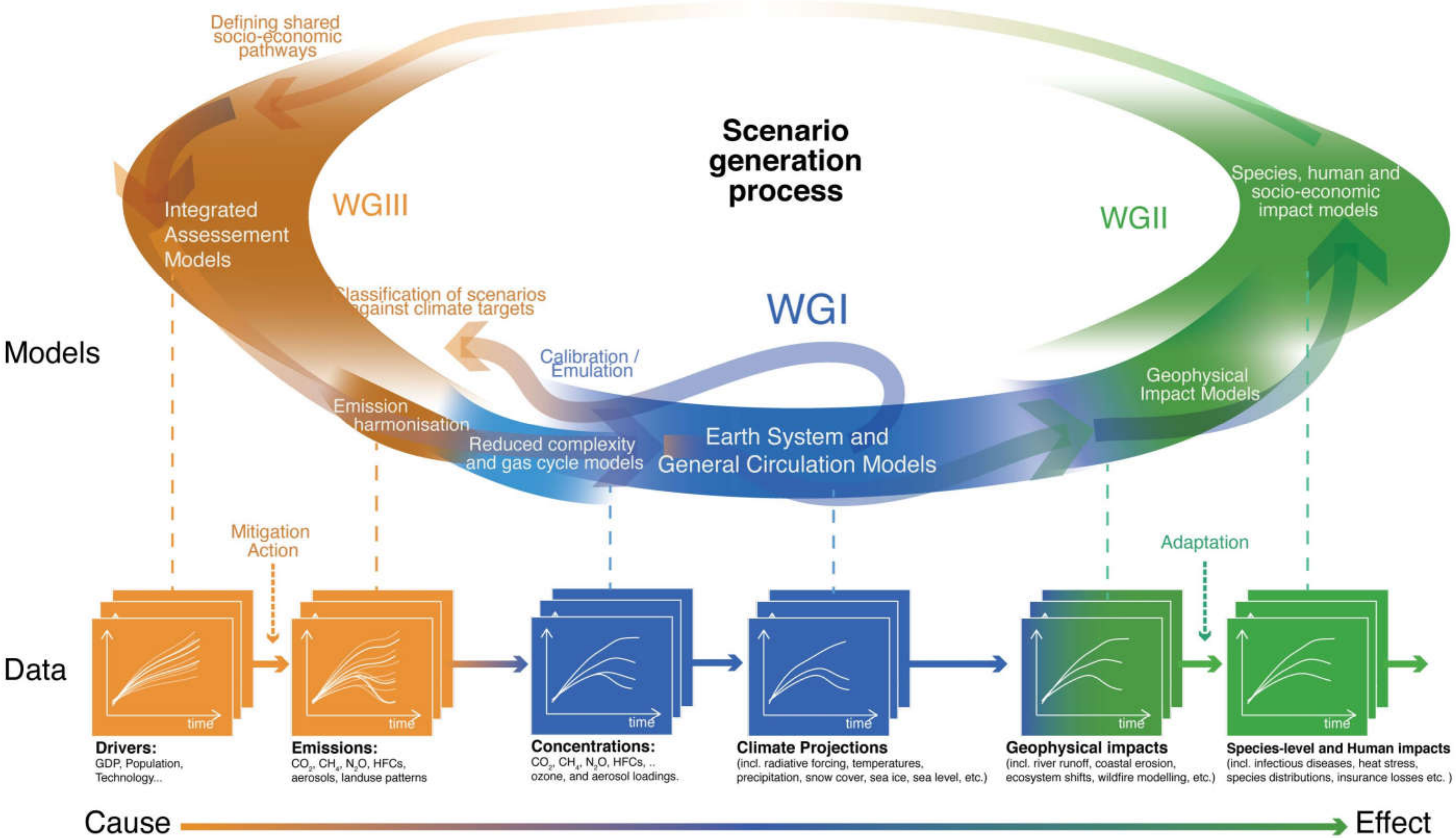

Sausen, Klimaänderung 1.1

Comparison of the range of fossil and industrial CO_2 emissions from scenarios used in previous assessments up to AR6.

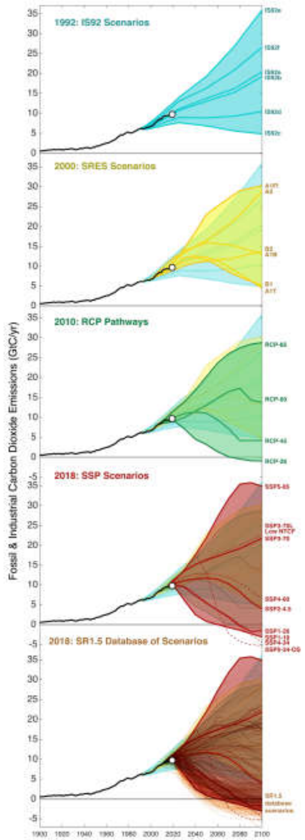

IPCC 2021, Chap. 1

Figure 1.28: Comparison of the range of fossil and industrial CO_2 emissions from scenarios used in previous assessments up to AR6. Previous assessments are the IS92 scenarios from 1992 (top panel), the Special Report on Emissions Scenarios (SRES) scenarios from the year 2000 (second panel), the Representative Concentration Pathway (RCP) scenarios designed around 2010 (third panel) and the Shared Socio-economic Pathways (SSP) scenarios (second bottom panel). In addition, historical emissions are shown (black line) (Chapter 5, Figure 5.5); a more complete set of scenarios is assessed in SR1.5 (bottom panel) (Huppmann et al., 2018). Further details on data sources and processing are available in the chapter data table (Table 1.SM.1).

Comparison of the range of fossil and industrial CO_2 emissions from scenarios used in previous assessments up to AR6.

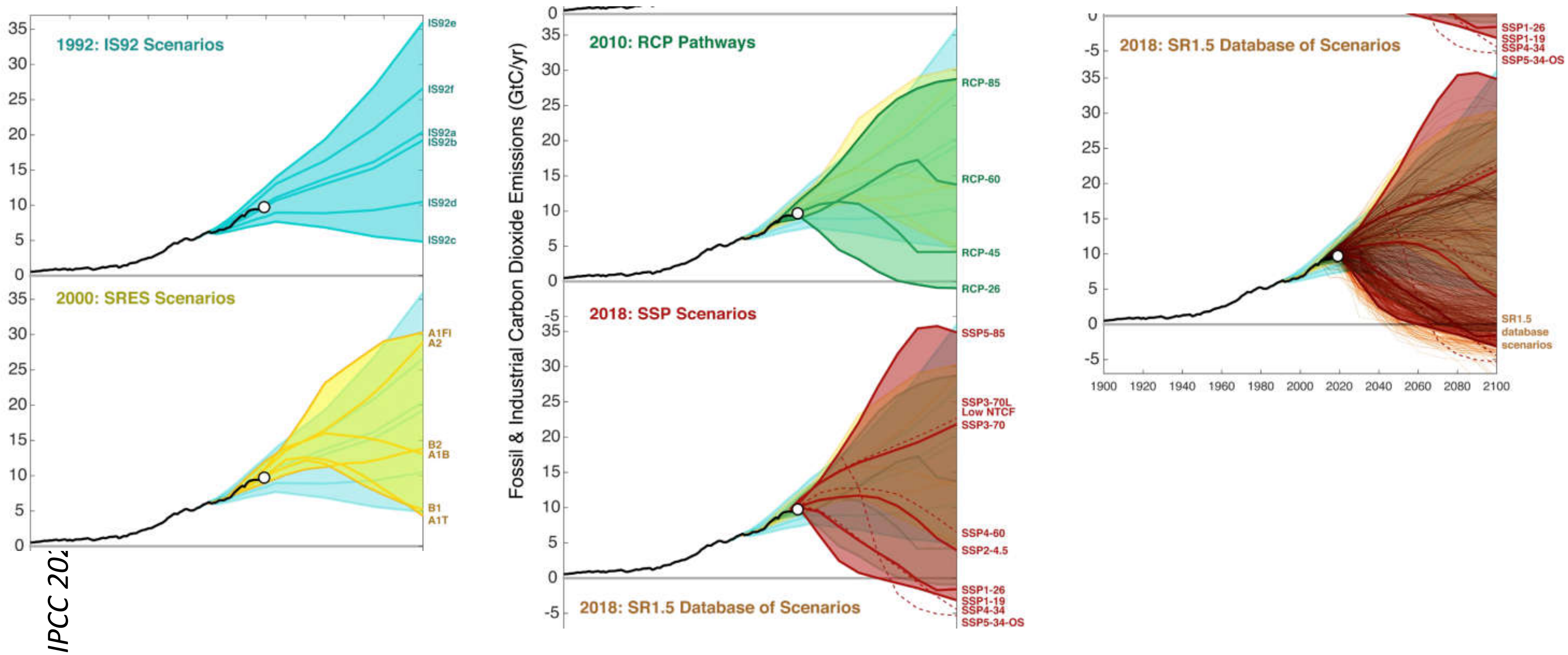

IPCC 20

Sausen, Klimaänderu

The Dimensions of Integration across Chapters and Working Groups in the IPCC AR6 assessment

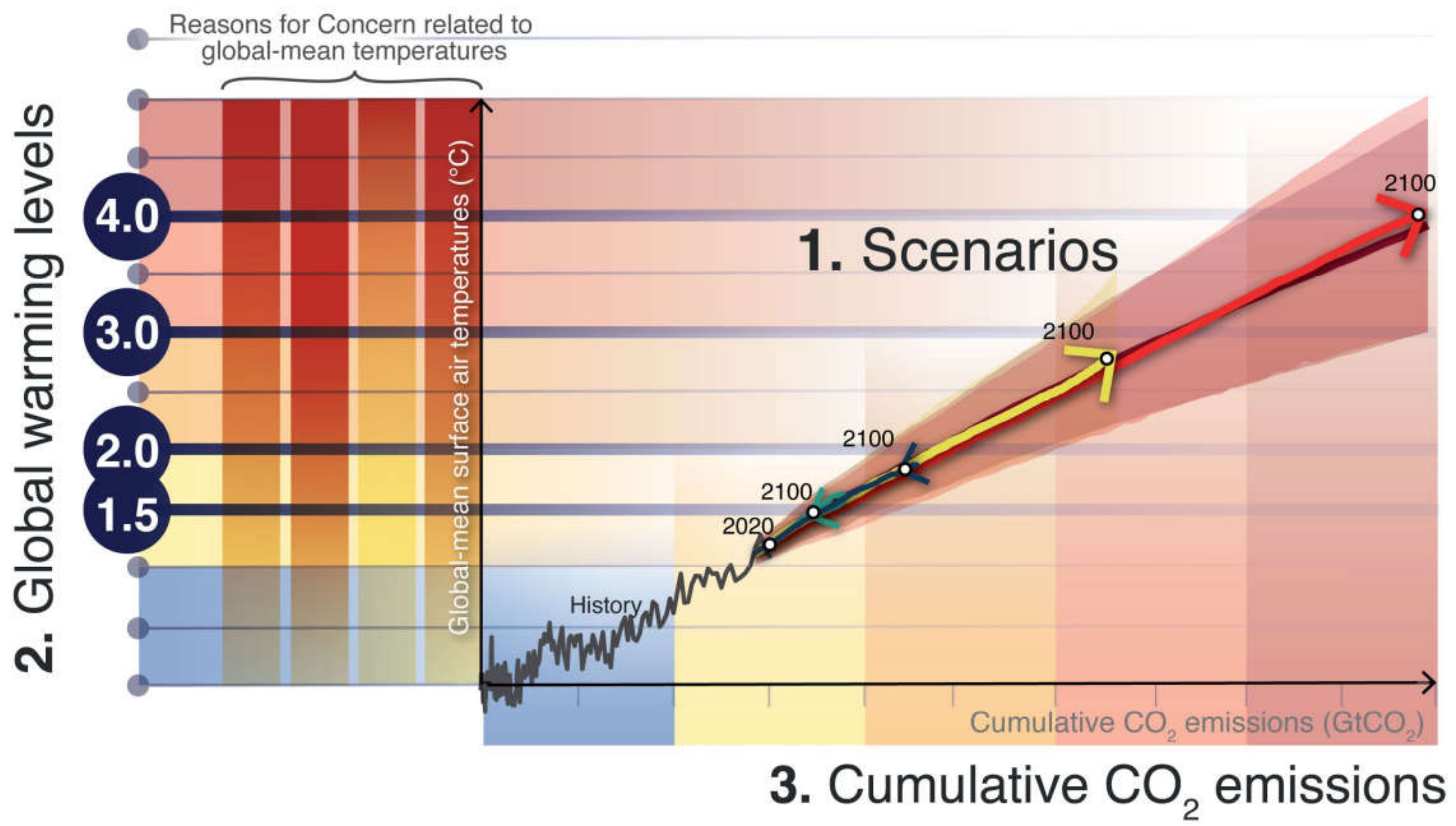

Figure 1.24: The Dimensions of Integration across Chapters and Working Groups in the IPCC AR6 assessment. This report adopts three explicit dimensions of integration to integrate knowledge across chapters and Working Groups. The first dimension is scenarios, the second dimension is global-mean warming levels relative to pre-industrial levels and the third dimension is cumulative CO_2 emissions. For the scenarios, illustrative 2100 end-points are also indicated (white circles). Further details on data sources and processing are available in the chapter data table (Table 1.SM.1).

IPCC 2021, Chap. 1

Sample elements of climate understanding, observations and models as assessed in the IPCC First Assessment Report (1990) and Sixth Assessment Report (2021)

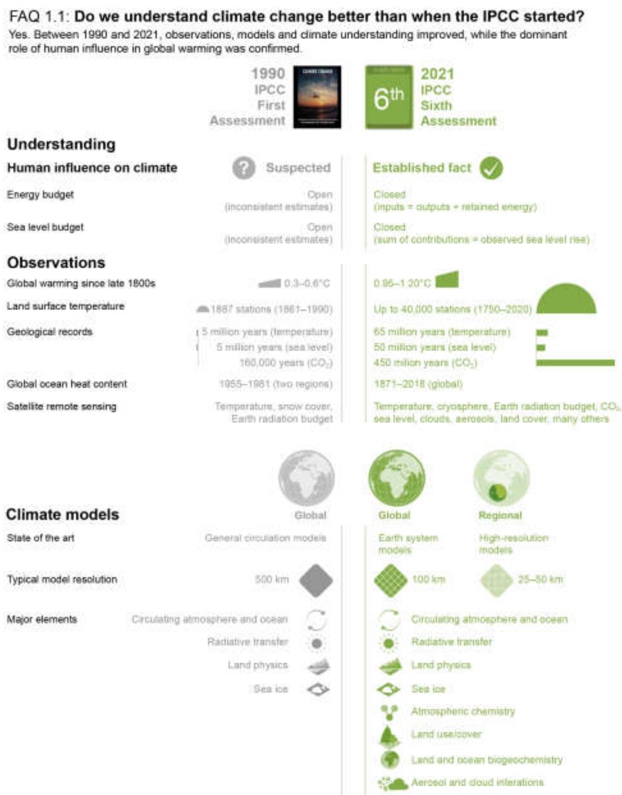

FAQ 1.1, Figure 1: Sample elements of climate understanding, observations and models as assessed in the IPCC First Assessment Report (1990) and Sixth Assessment Report (2021). Many other advances since 1990, such as key aspects of theoretical understanding, geological records and attribution of change to human influence, are not included in this figure because they are not readily represented in this simple format. Fuller explications of the history of climate knowledge are available in the introductory chapters of the IPCC fourth and sixth Assessment Reports.

IPCC 2021, Chap. 1

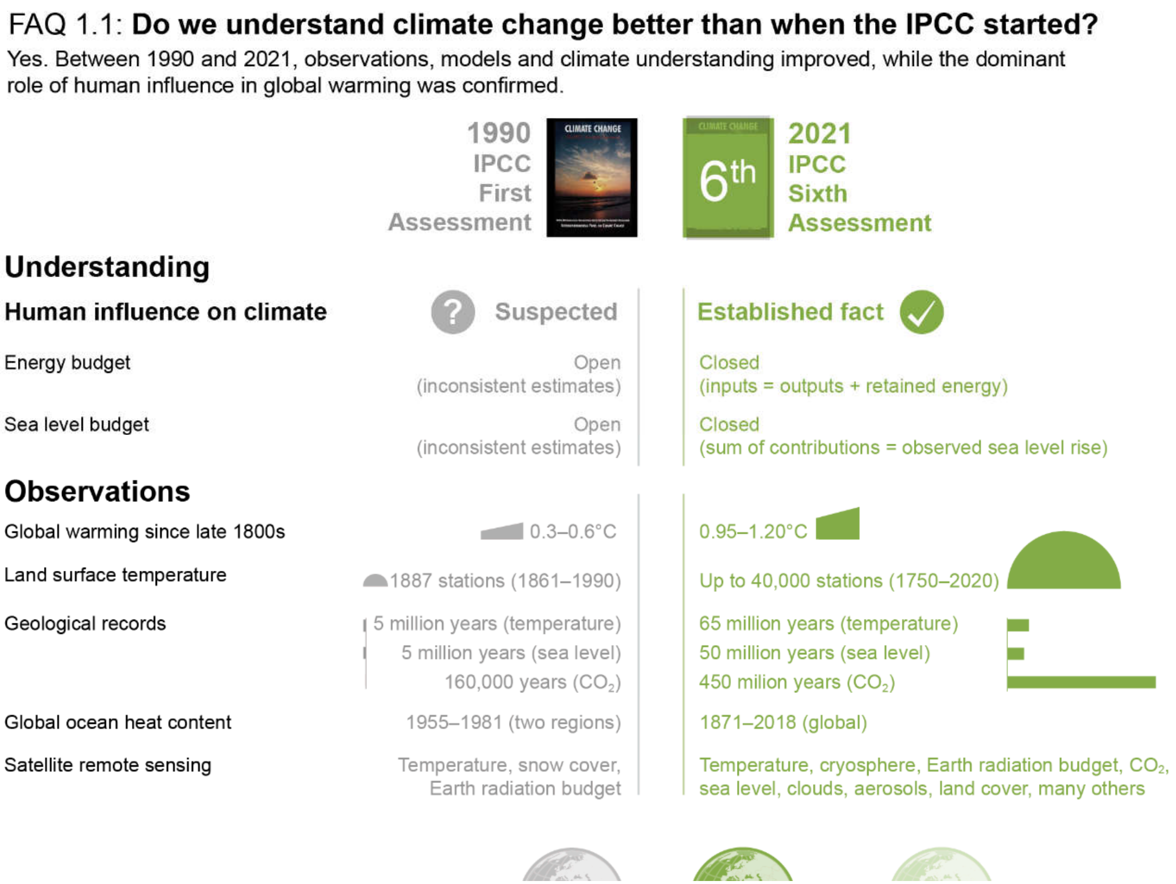

IPCC 2021, Chap. 1

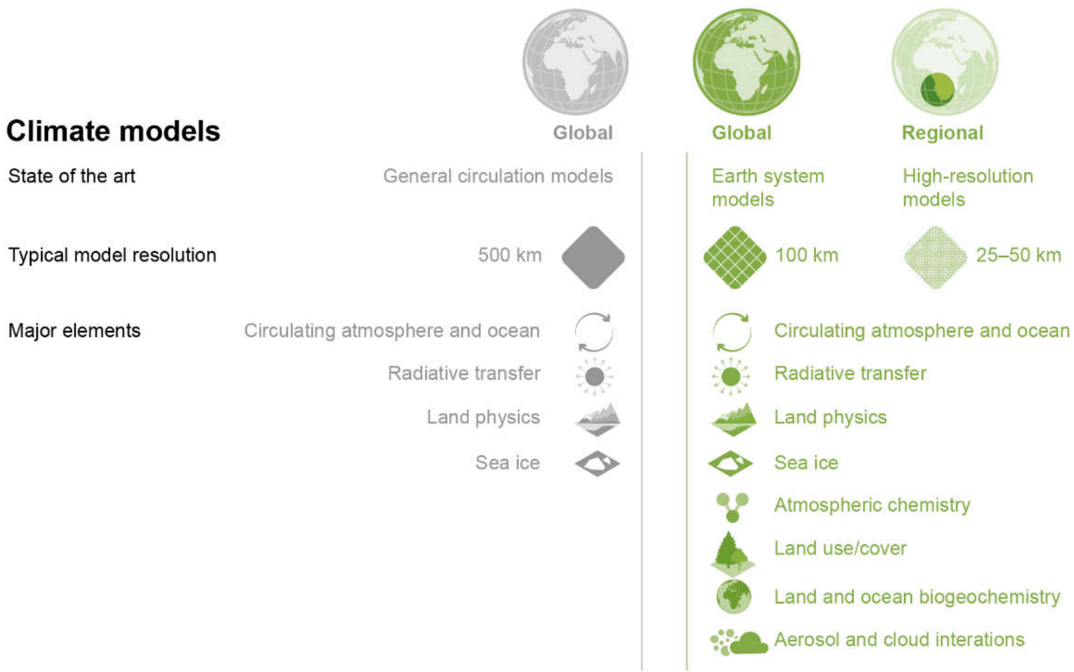

IPCC 2021, Chap. 1

Chapter 2: Changing state of the climate system

Nächste Vorlesung am 17. November 2021